REVISED PLANNING METHODOLOGY FOR SIGNALIZED

INTERSECTIONS AND OPERATIONAL ANALYSIS OF

EXCLUSIVE LEFT-TURN LANES

(DTFH61-92-00109)

PART-II: Models and Procedures
(Final Report)

Prepared for:

FEDERAL HIGHWAY ADMINISTRATION
(Washington, DC)

Prepared by:

Department of Civil Engineering
University of Maryland
College Park, MD 20742

1. Report Number	2. Government Accession No.	3. Recipient's Catalog No.

Title and Subtltle	5. Report Date
Revised Planning Methodology for Signalized Intersections and Operational Analysis of Exclusive Left-Turn Lanes: Models and Procedures	April, 1996
	6. Performing Organization Code

7. Author(s)	8. Performing Organization Report No.
G. L. Chang, C. Chen, X. Tao, E. Carter	

9. Performing Organization Name and Address	10. Work Unit No. (TRAIS)
Department of Civil Engineering University of Maryland College Park, MD 20742	
	11. Contract or Grant No,
	DTF'H 61-92-00109

12 Sponsoring Agency Name and Address	13. Type of Report and Period Covered
Turner-Fairback Highway Research Center Federal Highway Administration 6300 George Town Pike Mclean, Virginia 22 10 l-2296	Final Report October 1992-April 1996
	14 Sponsoring Agency Code

15. Supplementary Notes

FHWA contract manager, A. Barkawi, and engineers, S. Perez, H. Lieu all provided valuable assistance for the successful completion of this project.

16. Abstract

The study investigates the application of simulation along with field observations for estimation of exclusive left-turn saturation flow rate and capacity. The entire research has covered the following principal subjects: (1) A saturation flow model for protected phase that allows engineers to incorporate local-specific driving behavior in the analysis; (2) A permitted saturation flow model that accounts for the impact of driving behavior and traffic conditions at both the target and the opposing upstream intersections on the permitted saturation flow rate; (3) A queue length model for estimation of the resulting queue length under various phase schemes; and (4) A hybrid bay length impact model that provides engineers a convenient tool to assess the impact of various bay lengths on the left-turn capacity at both isolated and coordinated intersections. This report also describes the procedures for direct estimation of intersection capacity with simulation, including a set of rigorous statistical tests for simulation parameter calibration from field data.

17. Key Words	18 Distribution Statement
Exclusive Left-turn; Saturation flow rate	

19. Security Classif. (of this report)	20. Security Classif. (of this page)	21. Number cd Pages	22. Price

Reproduction of completed page authorized

TABLE OF CONTENTS

Chapter 1: Introduction

1.1   Research Objectives and Scope

The University of Maryland has been contracted by the Federal Highway Administration (FHWA) to develop traffic models and procedures for operational analysis of exclusive left-turn capacity at signalized intersections. The primary objectives of this contract are:

·   Develop specific recommendations on text, tables, and illustrative materials for revising the methodology used in the current Highway Capacity Manual (HCM) to analyze left-turns from exclusive lanes; and

·   Develop appropriate traffic models for analyzing the exclusive left-turn capacity under various signal phasings.

The work scope, as specified in the contract, consists of, as a minimum, the methodology for saturation flow estimation and adjustment factors which can realistically replicate traffic flow patterns under the following phasing schemes: protected, permitted, protected/permitted, and permitted/protected. The developed methodology addresses the effects of both left-turn bay length and the number of opposing lanes on capacity.

The entire project work was organized into the following tasks:

Task A: Review current research efforts

Task B: Development of initial models

Task C: Design of experimental plan

Task D: Site selection

Task E: Design of data collection plan

one can acquire sufficient local data to satisfy the extensive input needs of TRAF-NETSIM. With a well calibrated set of parameters one can exercise the simulation program to investigate the impacts of various critical factors on the left-turn capacity, including the distribution of driving populations, the start-up delay, and critical headways for permitted turns.

Research developed along the second line is to follow the current practice of computing the capacity with a sequence of equations, procedures, and adjustment factors. The research products for such applications include: a statistical model for protected saturation flow rate estimation, a hybrid model for permitted saturation flow rate analysis, a set of statistical equations for predicting the queue length at the start of a green phase under permitted, protected/permitted and permitted/protected phasings, two hybrid models for assessing the impacts of bay length on left-turn capacity under isolated and coordinated intersections. respectively. A detailed description of procedures for analyzing left-turn capacity under various phasings all with developed models has also been included as part of the products from the second research line.

The procedures developed under the second research line for capacity estimation intends to convey the vital concept that *"capacity is not a constant, but a stochastic variable depending significantly on the distribution of driving populations and resulting driving behavior. "* Neglecting such a local specific driving factor, one may seriously under or over estimate the left-turn capacity, especially at intersections having either a permitted phase or subphase. Hence, the proposed methodology intends not to rely on the results or factors from extensive field observations in various states or locations, but to take advantage of an effective simulation program along with minimum locally available data.

TRAF-NETSIM from field data, including a sequential analysis and statistical test. It also consists of an illustrative example for direct estimation of capacity with a simulation program such as TRAF-NETSIM.

Chapter 3 presents the procedures and research results from the development of a complex permitted saturation model. The developed model has taken into account all factors associated with the permitted flow, from both the upstream and downstream intersections. The number of opposing lanes, queue length of the opposing traffic, and the signal setting as well as coordination are all vital factors in the proposed permitted model for permitted saturation flow analysis. This chapter has also presented the design of experiments used to generate extensive data for model development and evaluation.

Chapter 4 discusses a saturation flow model for protected left-turns. It considers mainly the impacts of large vehicles as well as driving behavior discrepancy on the start-up delay and discharge headways which, in turn, affect the left-turn saturation flow rate. The product of research is a statistical model estimated with extensive simulated data which were generated with TRAF-NETSIM. A summary of field data analysis associated with left-turn characteristics and the use of such information to calibrate parameters in NETSIM also constitute a primary part of this chapter.

Chapter 5 illustrates three statistical models developed for estimating the opposing queue length at the start of a permitted phase or subphase. All those models were developed from the results of extensive simulation experiments which include the signal control impacts from both the upstream and downstream intersections. With such results, one can conveniently predict the time duration necessary to discharge all vehicles in a standing queue vehicles and compute the

Chapter 2: Direct Estimation of Intersection Capacity with TRAF-NETSIM

2-1   Introduction

As mentioned previously, simulation has evolved as one of the most powerful tools for traffic analyses, allowing engineers to effectively evaluate complex interactions between driver behavior, signal control, and geometric design. For someone familiar with computer applications, the best method for capacity estimation certainly is to simulate the intersection with a reliable simulation program, and directly obtain the number of vehicles passing the given intersection from simulation results. With such analyses, the impacts of those vital factors such as driving behavior and flow patterns can be realistically taken into account without making simplified assumptions. The fact that "capacity" of a traffic facility is not a constant, but a function of driving population, can also be better recognized.

To assist traffic engineers in using TRAF-NETSIM for capacity analysis, this chapter, with an emphasis on left-turn operations, consists of the following two parts: A detailed discussion of the calibration procedures for left-turn start-up delay and discharge headways with field data constitutes the core of Part I, followed by the presentation of procedures for use in capacity simulation. The presented procedures with minor modifications are applicable for use in both protected/permitted and permitted/protected left-turn operations.

This chapter is organized as follows: section 2.2 describes the procedures for calibrating start-up delay and discharge headways for protected left-turn analysis. Section 2.3 discusses some difficulties as well as the alternative of using field data in simulation of permitted phasing. Section 2.4 presents an example application of estimating a protected left-turn capacity with TRAF-NETSIM. Conclusions and recommendations constitute the core of the last section.

—   The discharging headways for up to the first 10 vehicles in the standing queue on a cycle-by-cycle basis; or up to the two standard deviations over the average queue length.

An implicit assumption in the above computation is that stable discharge headway can be achieved within the first 10 queue vehicles regardless of the standing queue length.

—   The mean and variance for each of the first 10 discharge headways over all observed cycles.

Note that to have a statistically meaningful comparison the field data for each computed headway must contain at least 30 observations to yield a statistically valid mean value for comparison.

Step 2:   <u>Stability test with respect to the sample observations from field data</u>

The purpose of this step is to ensure that the selected samples for the n-th headways are adequate for representing the local-specific driving population. Hence, one needs to perform the following test to determine if additional sample observations are necessary or not:

Hypothesis: $h(n, K) = h(n, K+\Delta K)$

Statistics: $$t_0 = \frac{h(n,K) - h(n,K+\Delta K)}{S_p \left(\dfrac{1}{K} + \dfrac{1}{K+\Delta K} \right)^{1/2}} \tag{1}$$

$$S_p^2 = \frac{(K-1)S_1^2 + (K+\Delta K - 1)S_2^2}{K + K + \Delta K - 2}$$

Reject the hypothesis, if $t_0 > t\,(\alpha,\, K+K+\Delta K-2)$, or $t_0 < (\alpha,\, K+K+\Delta K-2)$

Step 3:   <u>Computation of the average discharging headway and start-up delay for use</u>

in NETSIM

Given all computed mean headways for vehicles in the standing queue, one can obtain the

following weighted average headway for use in NETSIM:

$$\bar{h} = \frac{\sum_{n=1}^{N} h(n,K).K_n}{\sum_{n=1}^{N} K_n} \tag{2}$$

Where: $\bar{h}$ is the average discharge headway for use in NETSIM;

K_n is the sample size for the n-th vehicle in the standing queue

N is the average queue length or the first of 10 in the standing queue

With the average discharge headway, one can further identify the number of vehicles experiencing

the start-up delay, and compute the appropriate value for use in NETSIM. The following

statistical test can be used for identification of vehicles experiencing the start-up delay:

Hypothesis: $h(n, K) = \bar{h}$

Statistic: $t = \dfrac{h(n,K) - \bar{h}}{\left(\dfrac{S_1^2}{K_1} + \dfrac{S_2^2}{K_2} \right)^{1/2}}$ \hfill (3)

With the degree of freedom given by $v = \dfrac{\left(\dfrac{S_1^2}{K_1} + \dfrac{S_2^2}{K_2} \right)^2}{\dfrac{(S_1^2/K_1)^2}{K_1+1} + \dfrac{(S_2^2/K_2)^2}{K_2+1}} - 2$

Where: $h(n, K)$ is the n-th headways from K samples in the standing queue

organized in the same format as in Table 2-1.

Note that to minimize the output variation due to the stochastic nature of a traffic system, one should execute the simulation over a sufficiently long period so as to generate adequate sample observations from NETSIM.

Step 5: Analysis of output variability for TRAF-NETSIM

To ensure the adequacy of samples generated from NETSIM, one shall perform the same stability test as used in step 2 with respect to the average headway of each n-th vehicle in the standing queue. Note that even with detectors at the intersection, the current version of NETSIM is unable to capture the starting time of the first queue vehicle. Thus, one may not have the information of the first discharging headway and its start-up delay. However, as the total discharging time up to the n-th vehicle from the beginning of a green phase is available, one can choose the following alternate way to test the stability of the accumulated headways up to the n-th vehicle.

The hypothesis in Equation 1 for the n-th vehicle should be changed as follows:

Hypothesis: $$\sum_{n=1}^{N} h(n,K) = \sum_{n=1}^{N} h(n,K+\Delta K)$$

Step 6: Tests of statistical equality between the sequence of discharge headways generated from NETSIM and field observations

The purpose is to ensure that NETSIM can realistically replicate the field traffic conditions with the estimated start-up delay and average discharge headways. Since it is difficult for users to obtain the start-up delay and the discharging time of the first queued vehicle from the output of NETSIM, one shall start the test with respect to the series of accumulated discharging time up to the n-th vehicle. More specifically, the test is given as:

·   Perform the same pair-t test for each headway in sequence and identify those having significant discrepancy.

·   Investigate factors contributing to the discrepancy, such as a large fraction of buses, and remove them with additional sample observations from either field data or simulation output.

·   Restructure the data set and perform the same test until the results from NETSIM are consistent with those from field observations.

2.3   Calibration of Acceptable Gaps for use in TRAF-NETSIM

A rigorous calibration of acceptable gaps for permitted left turns is a complex task. Depending on the available information, one may either incorporate a local-specific model for permitted turns in TRAP-NETSIM, or simply replace the default distribution of gaps with field measured data. In the former case, the field observations for left turns must consist of both accepted and rejected gaps as well as key characteristics associated with each left-turner. The cost for collecting adequate field data at such a level of detail, however, is often prohibitively high. On contrast, the latter needs to have observed only those acceptable gaps. Since this chapter aims to take advantage of simulation functions in TRAP-NETSIM, our discussion with respect to acceptable gap calibration will focus on the latter scenario.

• Acceptable gaps embedded in TRAP-NETSIM for left-turners - In the current input file for NETSIM, the card type 145 consists of the following 10 types of default acceptable gaps for left-turning vehicles:

1. Compute both the average accepted gaps and their variance.

2. Compute the 95 percent likelihood intervals for the computed mean.

3. Employ a normal distribution with the computed mean and variance to generate those 10 types of critical gaps for use in Card Type 145.

4. Execute the simulation with the new set of acceptable gaps, and compute the permitted capacity from the simulation results (i.e., the actual number of vehicles successfully maneuver left turns).

5. Vary the mean of the employed normal distribution within its confidence interval (from step 2), and repeat the procedures from step 3 to step 4;

6. Organize all these simulated capacities from the sensitivity analysis, and compute the average capacity as well as it variance.

The result of capacity analyses with such an approach is consistent with the understanding that "capacity is not a constant, but a variable that changes with the distribution of driving populations."

2.4   Example Procedures for Estimating LT Capacity with TRAF-NETSIM

The procedures for direct estimation of left-turn capacity vary with the signal phasing plan. For instance, the network to be simulated should consist of both upstream and downstream intersections, if the target left turn has a permitted phase. In general, the following procedures are applicable for estimating of the left-turn capacity under various phasing plans:

Step 1:   Selection of an appropriate network for simulation

To minimize the simulation time as well as the data collection efforts, the network selected for simulation analysis of the left-turn capacity should be consistent with the signal plan. Under a protected phase, the saturation flow as well as capacity of left turns depends only on the green duration, start-up delay, and distribution of discharging headways. Hence, an isolated intersection consisting of the target left turn lane(s) should be sufficient to represent the interactions between left flows and all other affecting factors. For any phasing plan having a permitted subphase, (such as permitted, protected/permitted, and permitted/protected), it is essential to include the upstream intersection in the simulation (see Figure 2.2). This is due to the fact that the distribution of opposing traffic flows is the most critical factor in determining the filtering left-turning rate under permitted phase.

Step 2:   Calibration of key parameters in TRAF-NETSIM with field data

To reflect the driver behavior at the target site, one needs to calibrate local-specific parameters for use in simulation. These include start-up delay, queue discharging headways, the distribution of critical gaps under permitted turns, and the number of sneakers during the amber phase.

Step 3:   Set up the simulation input tile, based on the collected traffic flow distributions, roadway geometry conditions. and signal timings as well as chasing plans at all intersections in the selected network.

Note that the entry volume for each entry node of the selected network should be set to equal to the flow level at each boundary link.

Step 4:   <u>Increase the left-turning; flow in the input file and conduct an exploratory analysis to</u>

   <u>ensure the existence of saturated or oversaturated left-turn rate.</u>

Note that one effective way to check the saturated condition is to see if the queue vehicles exist on the left-turn lane during the entire simulation. With such a condition, the total number of vehicles successfully turning left during the simulation of one hour naturally reflects the available left-turn capacity under the given conditions as well as driving population.

Step 5:   <u>Execute the simulation over a period of one hour, and con-mute the total number of</u>

   <u>vehicles which have completed the left turns.</u>

The conversion of total left-turning vehicles into hourly flow rate is thus the left-turn capacity under the given geometric and signal control conditions.

It should be mentioned that driving populations, in realty, may vary substantially over different time periods, which, in turn, may affect the resulting capacity. To account for such variability, one may repeat the identical simulation process, but with different random number seeds. The result of each replication with a different set of random numbers basically represents the impact of driving population variation on the intersection capacity. The average of all replications will be a reasonable estimate of the actual left-turn capacity.

2.5   Closure

The chapter has presented the concept as well as the procedures for direct computation of left-turn capacity from simulation results. The proposed method allows potential users to realistically account for the impacts of various critical factors on the actual operational capacity. The distribution and variation of driving populations, which are extremely critical but remain

Chapter 3 Permitted Saturation Flow Models

3.1 Background

The presence of left-turning vehicles at signalized intersections tends to increase the accident potential, causing excessive delay and reduction of the intersection capacity. In practice, traffic engineers try to optimize the system operations with a variety of left-turn treatments, such as left-turn bays, exclusive left-turn lane(s), and different phasing strategies (i.e. permitted, protected, and protected/permitted).   Thus, appropriate procedures for evaluation of various left-turn treatments are essential.

In reviewing the literature, it was found that most existing methods for capacity analysis start with the estimation of saturation flow rate.   The capacity under various conditions can thus be obtained with appropriate adjustments of the effective green time, cycle length, and other related factors.   Some prominent studies in this area include: (1) Illinois method [15]; (2) Revised HCM draft [12,13,14]; (3) Canadian methods [17];   (4) Swedish approach [7,11,21]; and (5) Australian Road Research Broad procedures [1]. Except for the method by Machemehl, et al. [8], the core concept of all methods for permitted saturation flow rate was derived from the same queuing model of Poisson arrivals and exponentially distributed headways. Some critical factors, such as the number of opposing lanes, effects of signal control at the upstream intersection, and variation in driving populations, were either excluded from the formulation or represented with adjustment factors which are incompatible with the employed queuing theory. This is due to the fact that the inclusion of all critical factors along with realistic assumptions in the mathematical derivation will result in complex and intractable relations, considering the

Despite the flexibility of using statistical models from simulation results, it should be noted that the best set of parameters for a given set of observations does not necessarily reflect the actual interactions between traffic flow variables and all related factors, especially with the commonly-used linear regression. Hence, we propose the use of a hybrid model, which will capture all complex relations as much as possible with analytical formulations, and then model those intractable impacts from other related factors with statistical estimation methods such as regression. The advantages of such a method are: (1) the statistical model is non-linear in nature but allows one to perform the estimation with the simple linear method; and (2) such a formulation can include analytical results from some well-recognized studies in the literature which provide not only a better fit to the data but also an explainable relation from the operational perspective.

In this study we explore the use of such an approach for permitted saturation flow rate, as the collection of sufficient data for such a purpose will result in prohibitive costs and the complex interactions between permitted flow rate and all affecting factors are not analytically tractable. This paper is organized as follows: The nature of permitted left-turn operations and all factors affecting its filtering rate are presented in the next section. It is followed by a detailed description of simulation experiments and key parameter calibration in section 3. The model development along with estimation results is reported in section 4. Model stability analysis and concluding comments are summarized in the last section.

may vary dramatically, depending on the signal coordination 'between neighboring intersections.

In brief, critical factors associated with the permitted left-turn saturation flow rate include:

- opposing flow rate,

- number of opposing lanes,

- length of opposing lanes (i.e. the distance from the target intersection to its downstream intersection),

- speed distribution of the opposing flows,

- heavy-vehicle percentage of the opposing flows,

- start-up lost time and the distributions of queue discharge headways,

- turning radius of left-turn maneuvers,

- heavy-vehicle percentage of left-turn flows,

- start-up lost time and discharging headways of left-turn vehicles.

- signal settings in the target and its upstream intersections.

3.3 Experimental Design

As mentioned previously, due to both the difficulty in collecting sufficient permitted operation data and the resulting cost, we employ TRAF-NETSIM for generating all observations. To ensure that NETSIM can realistically simulate the traffic behavior, we have calibrated the following parameters with 12 field sites from three diierent states (i.e. Virginia, Delaware and Florida):

Key Variables in Simulation Experiments

Table 3.1 presents those variables selected as input variables in the simulation experiments for the permitted left-turn saturation flow analyses. Notably, to keep the saturated condition on the exclusive left-turn lane, one has to provide an oversaturated flow rate to the left-turn approach.

A. Two-Intersection Network

B. Link-Node Diagram for NETSIM
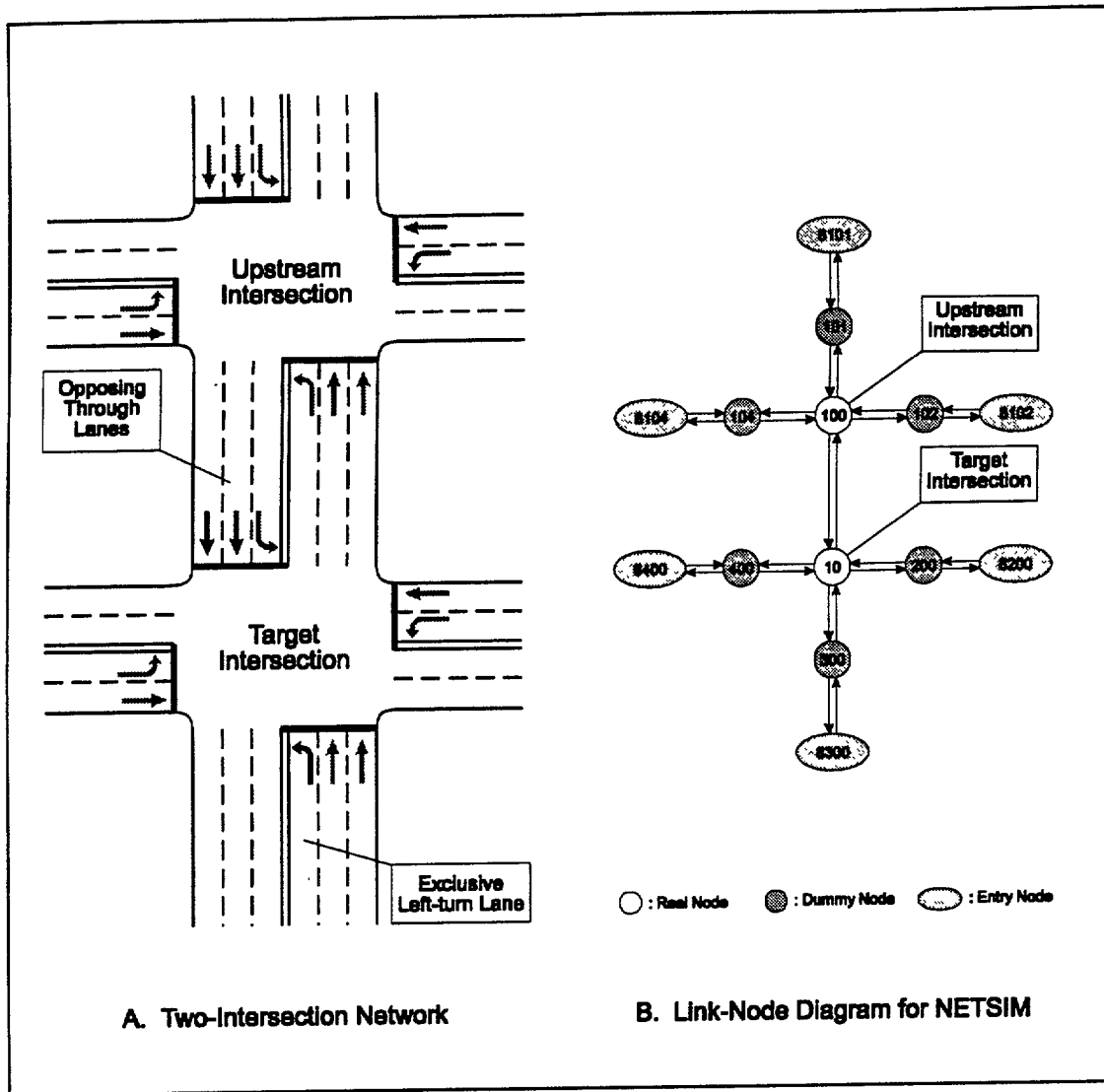
Figure 3.1 An example network used in the simulation experiments for permitted
left-turn saturation flows

Experimental Procedures

The experimental procedures for permitted saturation flows are summarized
below:

case of Tanner's formulation [16], has been selected as the principal term for use in regression analyses.

Drew's analytical model for the permitted left-turn saturation flow rate is based on the following assumptions:

- the opposing traffic is an uninterrupted flow, following a Poisson process,

- there is a continuous left-turn queue, and

- there are $(i+1)$ left-turn vehicles that can go through a gap, if the size of the gap is t and $t_{cr} + i{\cdot}h \leq t \leq t_{cr} + (i+1){\cdot}h$.

Grounded on the above assumptions, an analytical solution for permitted left-turn saturation flow was given by the following equations:

$$S = F_{OT} \cdot \sum_{i=0}^{\infty}(i+1)\cdot \Pr\{t_{cr} + i \cdot h \leq t \leq t_{cr} + (i+1)\cdot h\}, \tag{1}$$

and thus

$$S = F_{OT} \cdot \frac{\exp[-t_{cr} \cdot (F_{OT}/3600)]}{1 - \exp[-h \cdot (F_{OT}/3600)]}, \tag{2}$$

where: S = analytical estimation of the permitted left-turn saturation flow rate under F_{OT} opposing flow level (vph),

F_{OT} = total opposing through flows (vph),

t_{cr} = critical gap for left-turn vehicles (sec), and

h = mean of queue discharge headways (sec).

In this study, t_{cr} and h are set to 5.0 and 2.0 seconds, respectively, in Equation 2 to represent the base case.

This is due to the fact that TRAF-NETSIM uses 5.0 seconds as its default value for critical left-turn gap, and the results of some field surveys indicating that the average queue discharge headway is around 2.0 seconds. However, the variations caused by different t_{cr}'s and h's will be considered in the model with simulated data.

In addition to the above principal component, we have introduced a variable P, to indicate the platoon arrival time in reference to the beginning of the red phase at the target intersection. As illustrated in Figure 3.2, P can be computed with the following expression:

$$P = \frac{\text{mod}[(T + O_U), C] - g_T}{C},\tag{3}$$

where: P = indicator of signal progression,

T $= \dfrac{L_O}{V_a \cdot (5280/3600)}$ = estimated link travel time (sec),

V_a = the average flow speed

L_O = length of the opposing lanes (ft),

V_O = desired free flow speed of opposing flows (mph),

O_U = signal offset between the target and upstream intersections (sec),

C = signal cycle length at both intersections (sec), and

g_T = signal green time at the target intersection (sec).

As T represents a platoon's travel time from the upstream to the target intersections. Considering the signal offset at the upstream intersection (O_U), the platoon's actual arrival time should be $T + O_U$ at the target intersection. Furthermore, the arrival time is mod($T+O_U$, C) seconds after the beginning of a given cycle during which

3-13

Table 3.2 The correlation Coefficients of Key Variables for Permitted Left-Turn Saturation Flow Rate

Pearson Correlation Coefficients / Prob > |R| under Ho: Rho=0 / N = 300

	SPM	H	TCR	HL	NO	FOT	FOR	S	P
SPM	1.00000	-0.17439	-0.26945	-0.15066	-0.36708	-0.80733	-0.44564	0.88598	0.29728
	0.0	0.0024	0.0001	0.0090	0.0001	0.0001	0.0001	0.0001	0.0001
H	-0.17439	1.00000	-0.10885	0.02048	0.09051	-0.01131	-0.03665	-0.00682	0.07923
	0.0024	0.0	0.0597	0.7238	0.1177	0.8454	0.5271	0.9064	0.1711
TCR	-0.26945	-0.10885	1.00000	0.04080	0.03281	0.02741	-0.00699	-0.05624	-0.10818
	0.0001	0.0597	0.0	0.4814	0.5713	0.6363	0.9040	0.3316	0.0613
HL	-0.15066	0.02048	0.04080	1.00000	0.00456	0.02168	0.08237	-0.04809	-0.09933
	0.0090	0.7238	0.4814	0.0	0.9373	0.7084	0.1547	0.4066	0.0859
NO	-0.36708	0.09051	0.03281	0.00456	1.00000	0.44647	0.31087	-0.41374	-0.09754
	0.0001	0.1177	0.5713	0.9373	0.0	0.0001	0.0001	0.0001	0.0917
FOT	-0.80733	-0.01131	0.02741	0.02168	0.44647	1.00000	0.48679	-0.85620	-0.12952
	0.0001	0.8454	0.6363	0.7084	0.0001	0.0	0.0001	0.0001	0.0249
FOR	-0.44564	-0.03665	-0.00699	0.08237	0.31087	0.48679	1.00000	-0.51493	-0.14782
	0.0001	0.5271	0.9040	0.1547	0.0001	0.0001	0.0	0.0001	0.0104
S	0.88598	-0.00682	-0.05624	-0.04809	-0.41374	-0.85620	-0.51493	1.00000	0.22996
	0.0001	0.9064	0.3316	0.4066	0.0001	0.0001	0.0001	0.0	0.0001
P	0.29728	0.07923	-0.10818	-0.09933	-0.09754	-0.12952	-0.14782	0.22996	1.00000
	0.0001	0.1711	0.0613	0.0859	0.0917	0.0249	0.0104	0.0001	0.0

sufficient. This is mainly due to the design of scenarios in which only one left-turn lane was considered in all cases.

The estimation results of a preliminary linear model with all the above key factors are shown below:

$$S_{PM} = 959 + 0.49 \cdot S - 88 \cdot (t_{cr} - 5.0) - 264 \cdot (h - 2.0) - 64 \cdot N_O$$

$t-$value: (14.0) (12.9) (−13.1) (−12.6) (−6.4)

(4)

$$-0.37 \cdot \left(\frac{F_{OT}}{N_O}\right) + 139 \cdot P - 3.77 \cdot H_L,$$

(−9.5) (6.1) (−5.4)

R^2 value = 0.91, and

Number of observations = 300,

where: S_{PM} = permitted left-turn saturation flow rate (vph),

```
Plot of RES_M1*EST_M1.  Legend: A = 1 obs, B = 2 obs, etc.

        -+----+----+----+----+----+----+----+----+----+----+-
        |                                   |
   400 +                                    |        +
        |                                   |
        |                      A            |
        |        A    A    A       A        |
        |                 A         A        |
        |             A AA       A  A   A    |
   200 +    A    A  A   A   A     A    A      +
        |    A      AA   AA    A   A      A   |
   R    |    A  A   B A A A AA A   A  B    A   |
   E    |   AA      A BA AB A A AA AA   BAAA    AAA A A A B    |
   S    |   A B      AAB A  A AA BA BA ABA    A           |
   I    | A  A AAA B A  AAA ABA AA B B A ACBAAA  A  AAA   A A        |
   D  0 +-------A---A--ABAB--A-AA-A---AAA-AA--AABAA--A-A-AB-ABA---A-AABA-----------+
   U    |   A A    AAAB A   A  BB B  A   A BAACA AA A A         |
   A    |    B A B  ABA  AA AAA   BA C DAAA A AAB A       |
   L    |   A A A   AAA   A   C BC  A   BA  B A          |
        |   A  A AAA  A A  AA      A AAA A AB  A            |
        |   A  B AAAA   AA   A A A  A   A          |
  -200 +      AA AA      AA  AA     A                +
        |      A   A    A    A           |
        |         A              A        |
        |         A                       |
        |                                 |
  -400 +                                  +
        |                                 |
        -+----+----+----+----+----+----+----+----+----+----+-
       -200   0   200  400  600  800 1000 1200 1400 1600 1800 2000

                 ESTIMATED VALUE OF SPM
```
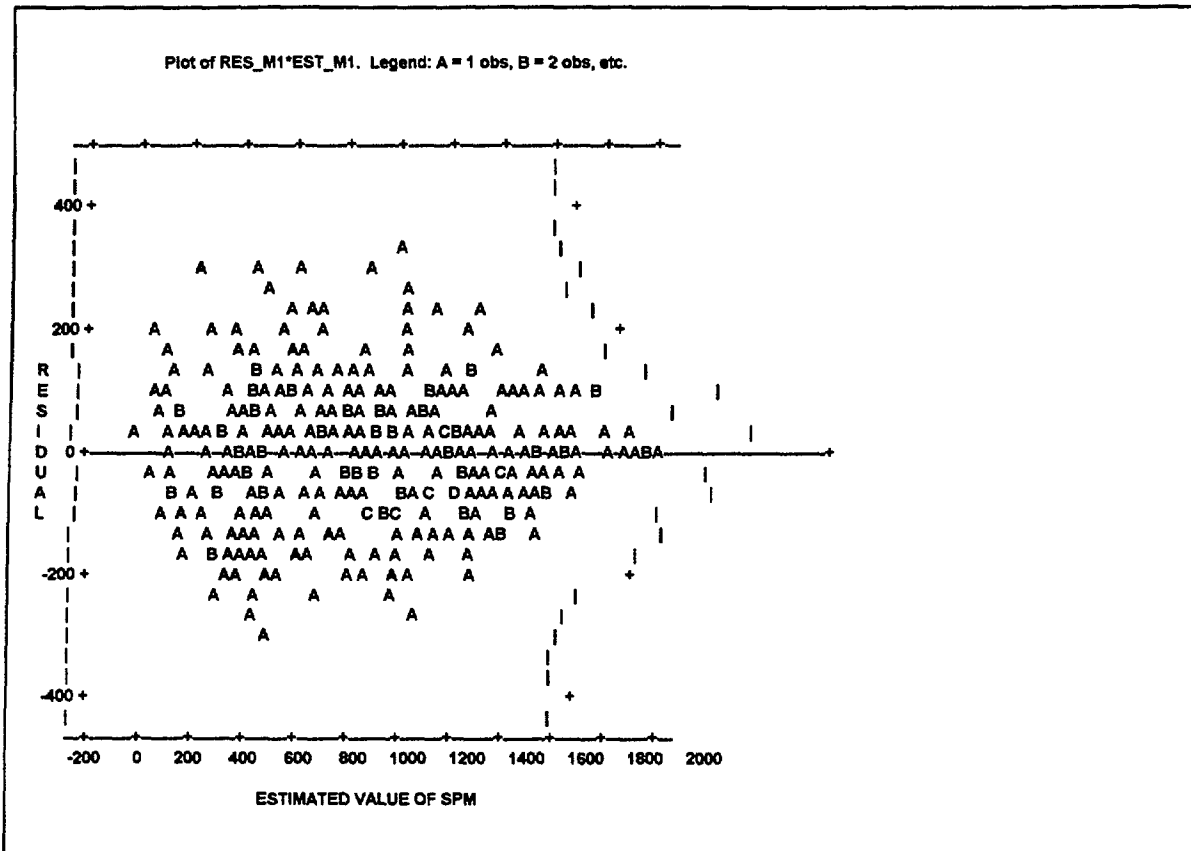
Figure 3.3 The plot of residuals versus estimated values for permitted saturation flows from the preliminary (linear) model with modeling data

the critical left-turn gap (t_{cr}), the heavy-vehicle percentage (H_L), the number of opposing lanes (N_O), and the opposing through flow rate (F_{OT}).

Notably, the terms $(h - 2.0)$ and $(t_{cr} - 5.0)$ are designed to reflect various types of driving behavior, where the h and t_{cr} may not equal 2.0 and 5.0 seconds, respectively. In addition to the total opposing through flow rate (F_{OT}), the model has also contained the term (F_{OT} / N_O), the opposing through flow rate per lane, to capture the compound effect.

Figure 3.3 presents the residual distribution that exhibits its consistency with some basic regression assumptions, such as a zero mean and constant variance. To further consider the convenience of applications, such a complex relation has been captured with a
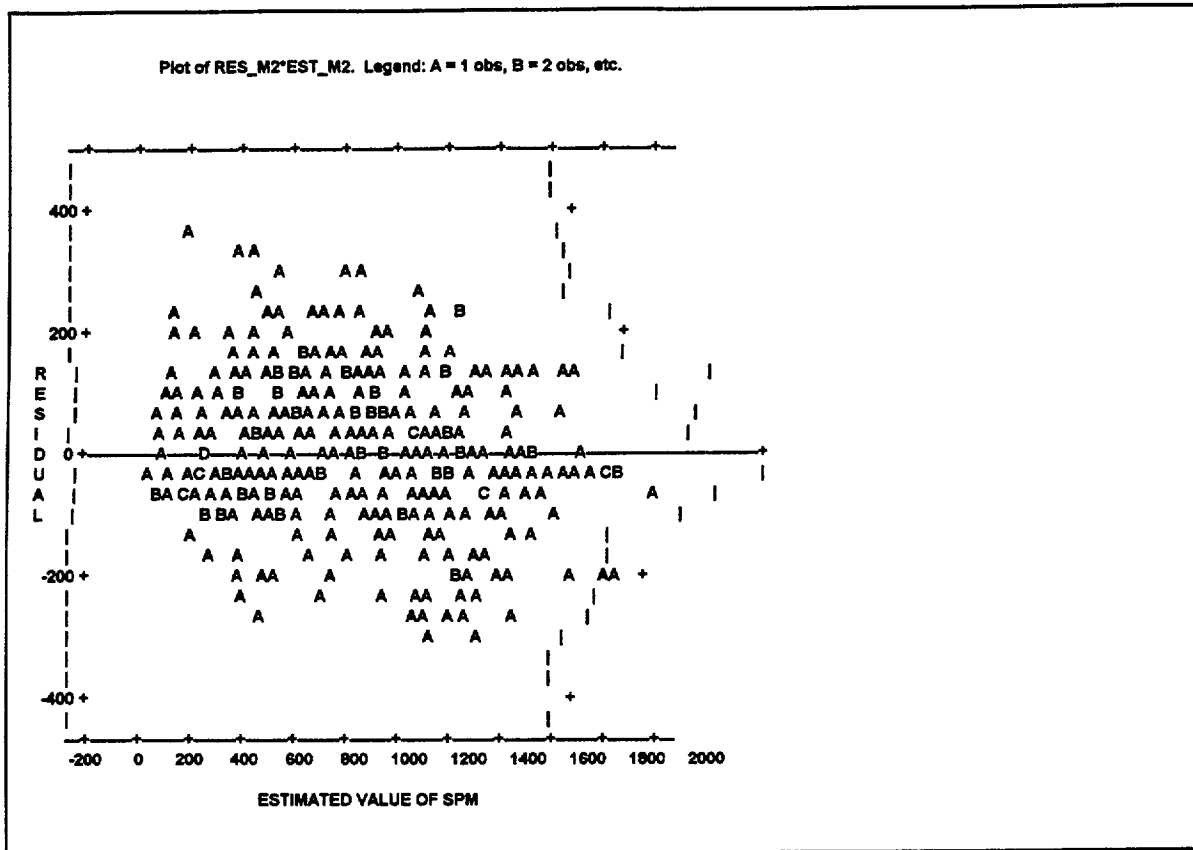
Figure 3.4 The plot of residuals versus estimated values for permitted saturation flows from the revised (log-linear) model with modeling data

promise of the proposed model structure. Figure 3.4 further presents the residual distribution of the revised multiplicative model that also shows an acceptable pattern.

To test the performance of the revised model, additional 50 simulation cases have been executed. Figure 3.5 illustrates the frequency distribution of the estimated errors based on the revised model (i.e. Equation 7). Most of the estimated values are within a reasonable range of their observed values.

Table 3.3 Summary of revised (log-linear) models and test results for permitted left-turn saturation flow rate

Basic Statistic	Pooled Data		First Subset		Second Subset	
No. of Observations	300		150		150	
R^2 Value	0.8864		0.9182		0.8478	
Model SS (df)	125.9004	(7)	74.5966	(7)	50.9138	(7)
Error SS (df)	16.1283	(292)	6.6468	(142)	9.1380	(142)
Total SS (df)	142.0287	(299)	81.2434	(149)	60.0518	(149)
Variable	**Parameter (t-Value)**		**Parameter (t-Value)**		**Parameter (t-Value)**	
Intercept	5.1914	(20.53)	4.9434	(16.34)	5.5604	(12.70)
$\ln(S)$	0.3221	(12.12)	0.3500	(11.05)	0.2806	(6.06)
$\ln(t_{cr}/5.0)$	-0.6284	(-9.61)	-0.5637	(-6.45)	-0.6655	(-6.70)
$\ln(h/2.0)$	-0.6871	(-8.03)	-0.7809	(-7.07)	-0.6017	(-4.51)
F_{OT}/N_O	-0.0005	(-6.27)	-0.0005	(-4.92)	-0.0006	(-4.10)
N_O	-0.0809	(-3.65)	-0.0611	(-2.18)	-0.1059	(-2.96)
P	0.3150	(7.17)	0.3622	(6.37)	0.2926	(4.19)
$\ln(1+0.01H_L)$	-0.5717	(-3.60)	-0.5047	(-2.33)	-0.6623	(-2.78)
Testing Statistic	**Chow Test -- Testing the stability of model parameters**					
F^* Statistic	0.7728					
$F_{.05, v1, v2}$	1.9711					
$H_0: b_1 = b_2$	Accept					

Performance Evaluation

Although in conducting this study we have collected permitted data from several field sites, the results are not sufficient for use in model evaluation. This is due to the fact that all such sites having heavy left-turn flows have been changed to either protected or protected-permitted control. Those currently under permitted control all have the flow rate far under the saturation level. Hence, we have selected the simulated scenarios which cover a wide range of traffic conditions for model comparison and performance evaluation.
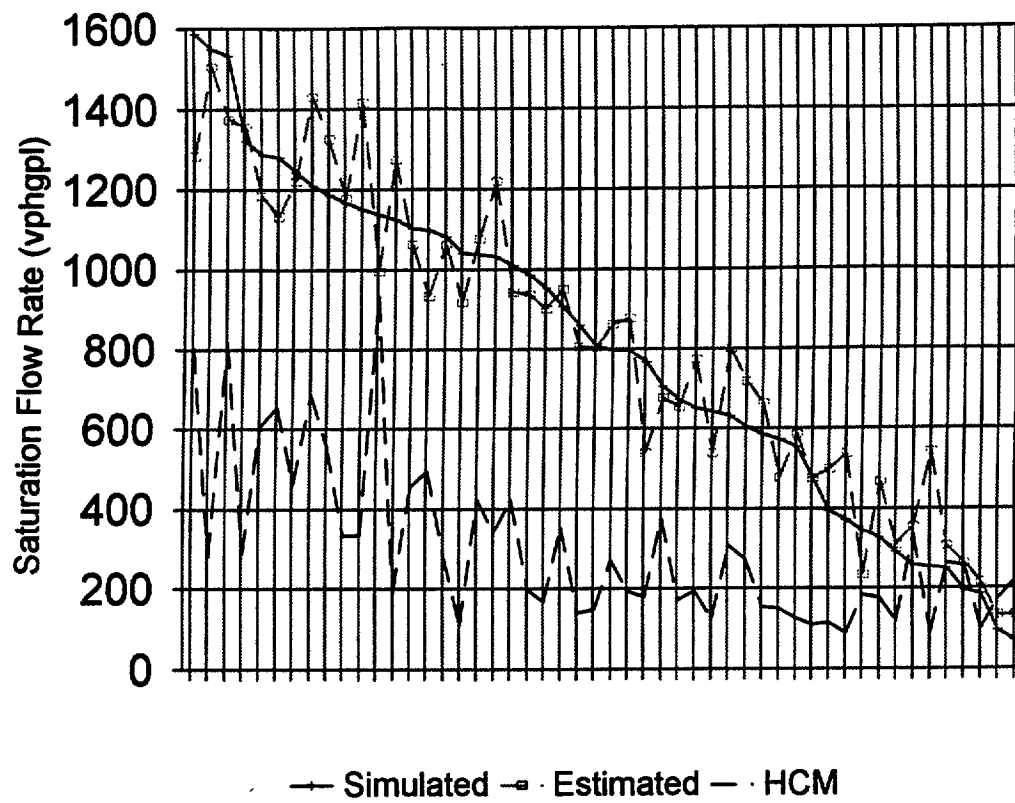
Figure 3.6 Performance Comparision with Simulated Scenarios

- Although the developed model does not have the mathematical elegance as with analytical formulations, it is capable of realistically incorporating all associated factors and their collective impacts in real world operations,

- Based on the results of the Chow stability test, the proposed model shows that both the model structure and the parameters are quite stable and independent of sample size.

- The use of simulation methods not only circumvents the need of extensive field data which often results in prohibitive costs, but also effectively yields some vital information that cannot be accurately measured from field observations.

- To further understand the characteristics of left-turn saturation flows, it will be necessary to investigate:

  - the protected left-turn saturation flow models for exclusive double and triple left-turn lanes,

  - the left-turn flow filtering rate during the transition period of the protected/permitted and permitted/protected signal phasings, and

  - the effects of U-turning vehicles on the left-turn saturation flows.

- To accomplish the left-turn capacity analysis, at least two more issues should be taken into account:

  - a reliable queuing model, for estimating the average queue length on the opposing through lanes and for computing the effective green time for left-turning vehicles; and

  - the effect of various bay lengths on the left-turn capacity under both protected and permitted phasings.

Chapter 4   Protected Saturation Flow Models

4.1 Introduction

This chapter presents an estimation model for the left-turn saturation flow rate on an exclusive lane under protected phasing. It contains the following sections:

Section 4.2 introduces the definitions and the factors associated with protected left-turn saturation flow rate.   Section 4.3 presents the results of field data analysis from four states. Section 4.4 describes the design of simulation experiments, including the key input variables and the experimental procedures.   Finally, Section 4.4 reports the model development process and the research conclusions.

4.2 Definition of Protected Left-Turn Saturation Flow Rate

In review of the literature, it can be found that there are several different definitions for saturation flow rate. For instance, the HCM describes the saturation flow rate as the flow, in vehicles per hour, which can be accommodated by the lane group, assuming that the green phase is always available to the approach. The Canadian method [1, 2] defines saturation flow as the queue discharges from the stop line of an approach lane, expressed in passenger-car units per hour of green. The Australian approach [3] states the saturation flow as the maximum constant departure rate from the queue during the green period, expressed in through-car units per hour.

This study intends to follow the HCM concept and defines the protected left-turn saturation flow rate as:

conditions, the current HCM provides only a simplified adjustment constant of 0.95 for exclusive left-turn saturation flow rate.

This is based on the assumption that driving behavior in terms of start-up delay and discharging headways will not either be a critical factor or vary substantially over different locations. Such an assumption, however, is quite inconsistent with field observations, and the average discharging headway is indeed one of the most critical factors dictating the achievable maximum flow rate. Some of field observations with respect to these two factors are reported in the next section.

4.3 Field Data Analysis

Tables 4.1 to 4.4 summarize the field observations from four different states, containing the left-turn discharging headways up to the 10th vehicle in the queue. The results of analysis were based on those sites having either protected only or the protected subphase of protected-permitted phasing.   To explore the necessity of incorporating a local-specific driving factor in the saturation flow analysis, we focus the analysis on the following issues:

The variability of start-up delays within and between those four states

The variability of saturation headways within and between those four states

The variability of overall queue discharging patterns

Table 4.2 (Florida)

Summary of left-turn discharging headways up to the 10th queued vehicle

unit=second

nth vehicle	1	2	3	4	5	6	7	8	9	10
Site A	2.63	2.3	2.09	1.95	1.81	1.76	1.89	1.92	1.73	1.66
(N)	(43)	(42	(39)	(32)	(23)	(19)	(14)	(11)	(10)	(5)
Site B	3.46	2.59	2.21	2.09	1.99	2.11	2	1.95	2.03	2.08
(N)	(54)	(52	(50)	(47)	(47)	(44)	(41)	(36)	(30)	(25)
Site C	3.72	2.44	2.14	2.1	1.94	1.97	1.83	1.77	1.84	1.97
(N)	(51)	(51)	(51)	(51)	(51)	(51)	(50)	(50)	(50)	(47)
Site D	3.34	2.22	2.35	2.21	1.96	2.05	1.92	2.04	1.89	1.97
(N)	(49)	(49)	(48)	(47)	(47)	(46)	(45)	(44)	(37)	(32)
Site E	3.17	2.48	2.51	2.35	2.11	2.32	2.06	1.61	1.65	1.74
(N)	(27)	(27)	(27)	(24)	(24)	(23)	(19)	(16)	(14)	(11)
Site F	2.28	2.41	2.3	2.28	2.19	2.16	2.21	2.04	2.14	2.25
(N)	(33)	(31)	(29)	(28)	(26)	(20)	(14)	(9)	(7)	(3)
Site G	3.06	2.6	2.26	2.14	2.21	1.8	1.91	1.91	1.77	1.86
(N)	(48)	(48)	(48)	(48)	(48)	(44)	(43)	(40)	(32)	(22)
Average	2.78	2.44	2.25	2.15	2.03	2.01	1.92	1.89	1.86	1.95

* (N) denotes the number of observations

Table 4.3 (Nevada)

Summary of left-turn discharging headways up to the 10th queued vehicle

nth vehicle	1	2	3	4	5	6	7	8	9	10
Site A	3.24	2.27	2.39	1.98	2.22	2.08	0	0	0	0
(N)	(36)	(36)	(35)	(31)	(33)	(1)	-	-	-	-
Site B	2.26	2.36	2.18	2.17	2.13	2.01	1.92	1.84	1.89	1.92
(N)	(42)	(42)	(42)	(42)	(42)	(41)	(39)	(35)	(34)	(33)
Site C	2.77	2.63	2.32	2.27	2.11	2.12	1.84	1.92	1.83	1.78
(N)	(51)	(51)	(50)	(46)	(40)	(34)	(32)	(22)	(19)	(16)
Site D	3.1	2.89	2.45	2.34	2.45	2.53	0	0	0	0
(N)	(40)	(40)	(39)	(38)	(32)	(22)	-	-	-	-
Average	2.82	2.55	2.33	2.20	2.18	2.17	1.88	1.87	1.87	1.87

(N): The number of observations

Tables 4.3 and 4.4 have summarized the discharging headway distributions from those sites in Nevada and Maryland, respectively. The overall patterns with respect to start-up delays seem quite similar to those in Delaware and Florida, where the discharging headways of the second and third queued vehicles from those sites in Nevada vary within an interval of 2.27 ~2.89 seconds, and 2.18 ~ 2.45 seconds, respectively. Its first queue discharging headways, however, differ significantly, ranging from 2.26 seconds to 3.24 seconds. This is possibly due to the substantial difference in geometry at those sites, as some sites are quite large and have triple left-turn lanes in more than two approaches. Such a plausible explanation is consistent with observations at Maryland sites, where the geometric conditions as well as volume levels are quite similar between those three sites. Hence, the discharging headways of all first three vehicles have varied within a very small range. For instance, the first discharging headway ranges from 2.92 to 3.1 seconds; the second and third headways vary from 2.24 to 2.44 seconds, and 2.06 to 2.38 seconds, respectively.

Start-up delay variation between states

As the first three vehicles in queue are more likely to experience significant start-up delay, we have compared such observations at the above four sites. The comparison results are reported in Figure 4- 1. With a simple variance analysis, one can further observe the following facts:

- The start-up delay is progressively reduced from the first vehicle to the subsequent vehicles in the queue.

- The first vehicle generally experienced a relatively long start-up delay, and the magnitude of such delay varies significantly with the differences in location.

- The discharging headway of the second vehicle in the queue is relatively stable across different states, varying in a small range (i.e., 2.33 to 2.55 seconds).

- The stability of discharging headway seems to increases with the queue position of vehicles. For instance, the average discharging headways of the third vehicle among those four states are distributed in an interval of 0.19 seconds (from 2.14 to 2.33 seconds), a statistically insignificant range.

Note that unlike the use of sensors for headway measurement where it is often difficult to identify the position of first queued vehicle, we have employed two video recorders to collect such information, including the precise start-up time of the green phase and the time at which the first vehicle has passed the stop line.

Saturation discharging headway variation within each state

Some existing methods have recommended the use of saturation headway (i.e., maximum constant departure rate) to compute the saturation flow rate. The selection of such a headway, however, is a quite difficult issue, as it may vary dramatically due to the difference in driving behavior. As such a saturation discharging headway is most likely to start from the range of the 4th to 6th queued vehicle. we have explored the variation of those discharging headways within and between states in the following analysis.

Sites E and F – As only a very few observations at these two' sites have queues over six vehicles, the steady discharging headway is thus likely to he between the 4th and the 6th vehicles. At Site E, such headways varies between 1.9 to 2.1 seconds with an average of 2.04 seconds. In contrast, those at Site F vary between 1.86 and 2.07 seconds with an average of 1.95 seconds.

In summary, the saturation headway in Delaware varies substantially from one location to the other, depending on the driving population. Care should be exercised if the discharging headway is selected for computation of saturation flow rate.

Florida:

Site A – Drivers observed at this site are all quite aggressive. The discharging headways of the 4th to 6th vehicles in the queue vary between 1.76 to 1.95 seconds with an average of 1.85 seconds. AU subsequent vehicles were mostly discharged around an average of 1.83 seconds.

Sites B and C – These two sites have quite congested traffic conditions. In most observed cycles there were more than 10 vehicles in the queue. The average discharging headways of the 4th to 6th queued vehicles at Site B and Site C are 2.03 seconds and 1.91 seconds, respectively. The remaining queued vehicles at Site B and Site C were discharged at an average of 1.99 seconds and 1.85 seconds respectively.

The existence of such a substantial difference in delay indicates that drivers at Site C are apparently more aggressively than those passing Site B.

drivers from Site C were mostly from a shopping mall. Thus, the discharging headway of the 4th to 6th vehicles in queue are quite different, ranging from 1.83 seconds to 2.38 seconds. As shown in Table 4.4, the average of such a headway at Site A is 1.84 seconds, but is 1.88 and 2.25 seconds, respectively at Sites B and C. Such a difference is also reflected in the discharging pattern of the remaining vehicles in the queue.

<u>Saturation discharging headway variation between states</u>

Figure 4.2 has presented the comparison of the average discharging headways for the 4th to 6th vehicles in the queue in the above four states. With a simple variance analysis, one can conveniently reach the following conclusions:

- The discharging headways of the 4th to 6th queued vehicles are statistically unequal across those four states, with an exception of the 4th queue vehicle's discharging headway between Florida and Delaware.

- Nevada which has most non-local drivers clearly has longer discharging headways than the other states.

- The discharging headway is progressively reduced from the 4th to the 6th vehicles in queue, except that in Maryland mainly due to a substantial difference in observed samples between its sites.

- The observed Maryland drivers are more aggressive than those in other states, as they are within a large metropolitan area.

- The discharging headways of the 4th to 6th queue vehicles are relatively stable, compared to the first three vehicles in the queue. Hence, the

Figure 4-3: Field observations of Discharging Headway Patterns

Delaware
Flordia
Nevada
Maryland

Discharging headway (second)

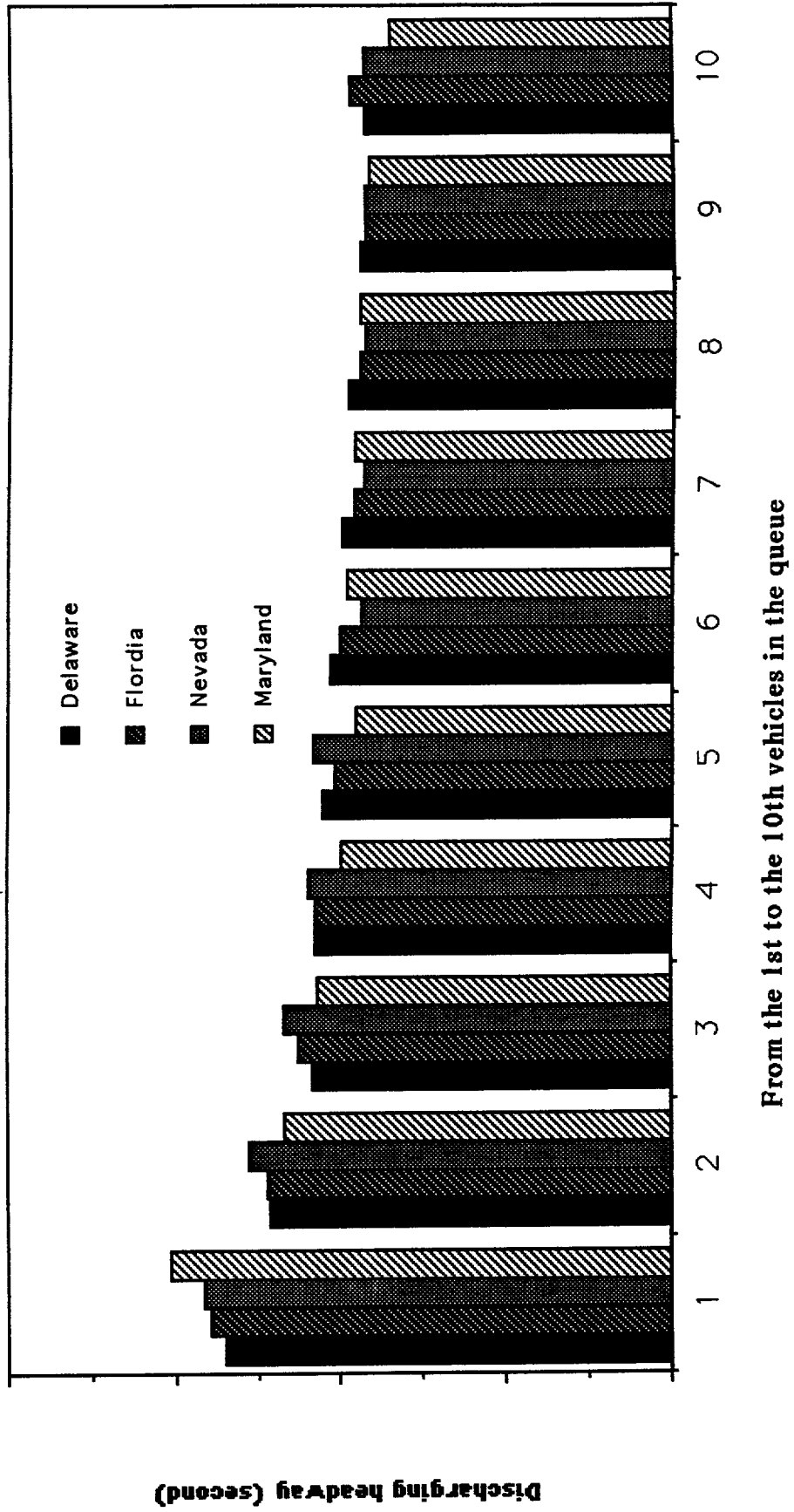From the 1st to the 10th vehicles in the queue

4-15

Table 4.5 illustrates those factors which have been used as input variables in the simulation experiment for protected left-turn saturation flow rates after extensive exploratory analyses. To ensure the saturated condition under protected phasing, the simulation experiment always generates an oversaturated flow rate to the exclusive left-turn lane. All other movements in the simulation experiments, for computation convenience, are assumed to have no flow.

Table 4.5 The variables selected for use in the simulation experiments for protected left-turn saturation flow rate

Independent Variable			Lower Bound	Upper Bound	Increment
h	Mean of Queue Discharge Headway	(sec)	1.6	2.6	0.2
d	Mean of Start-Up Lost Time	(sec)	2.0	4.5	0.5
L_L	Length of Exclusive Left-Turn Lane	(ft)	500	4000	500
V_L	Desired Speed of Left-Turn Flows	(mph)	25	50	5
H_L	Heavy-Vehicle Percentage of Left-Turn Flows	(%)	0	30	3
C	Signal Cycle Length in Target Intersection	(sec)	60	120	10
g/C	Green Ratio to Signal Cycle Length		0.4	0.8	0.1
g_{PT}/g	Protected Green Ratio to Total Green Time		0.3	0.6	0.1
Dependent Variable			Relationship		
g	Signal Green Time	(sec)	$g = (g/C)\,C$		
r	Signal Red Time	(sec)	$r = C - g$		
gPT	Green Time for Protected Left-Turns	(sec)	$gPT = (gPT/g)\,g$		
gPM	Green Time for Through Movements Only	(sec)	$gPM = g - gPT$		

Note: 1   The values of gPT, gPM, and r should meet the following regulations: 20 z gPT z,30, 20 z, gPM z,40, 20 z, r z,60, and gPT-gPM z10.
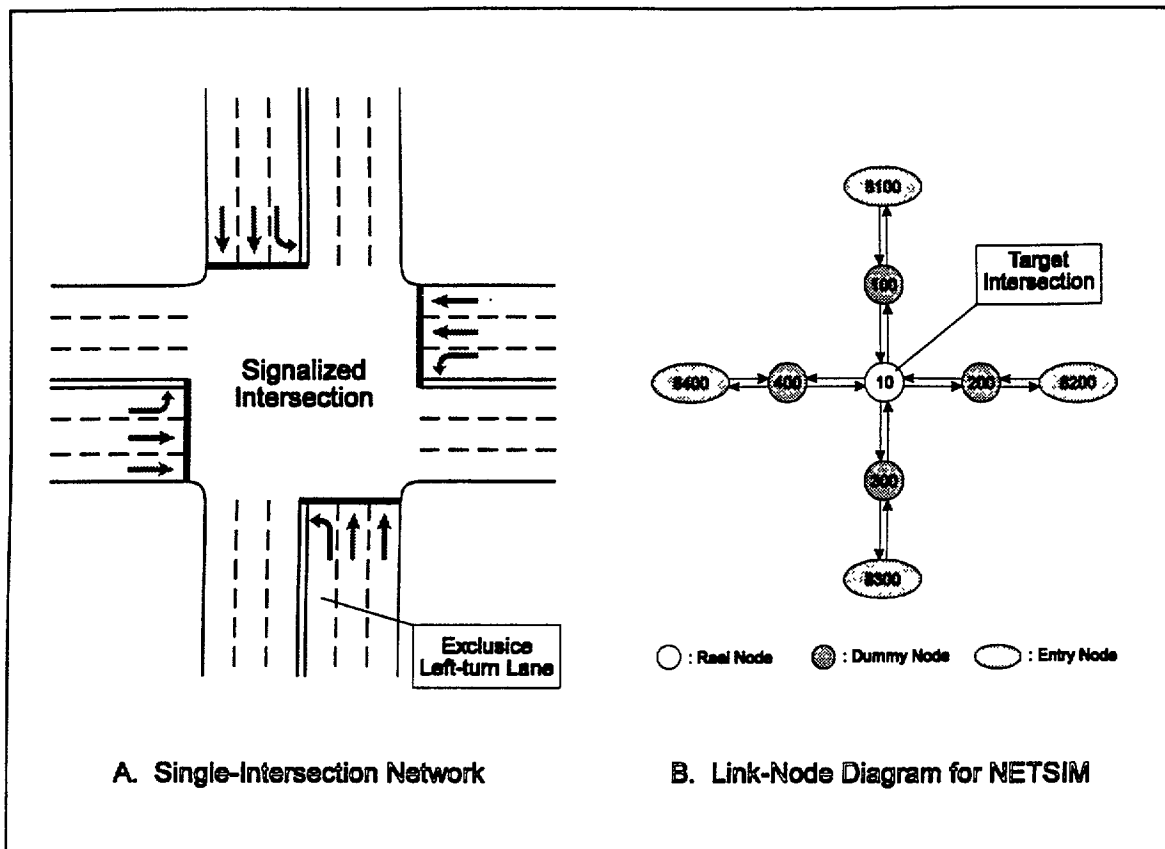
Figure 4.4 An example network used in the simulation experiments for protected left-turn saturation flows

4.5 Model Estimation and Testing

Table 4.6 summarizes the results of correlation analysis based on 300 observations from simulation experiments. The statistical significance test indicates that the protected left-turn saturation flow rate is likely to be a function of the average queue discharge headway (h) and the heavy-vehicle percentage of left-turn flows (H_L). All other variables appear to have insignificant impact on the left-turn saturation flow rate. Those include the average start-up lost time (d), the length of left-turn lane (L_L), the desired speed of left-turn flows (V_L), the signal cycle length (C), the green times (g_{PT}), and the

where: S_{PT} = protected left-turn saturation flow rate (vph),

               h = mean of queue discharge headway (sec), and

            H_L = heavy-vehicle percentage of left-turn flows (%).

As expected, both the R^2 value and the t-value for each parameter indicate the promising properties of the preliminary model. The sign of each parameter is consistent with the relations shown in the correlation analysis. The implication is that the protected left-turn saturation flow rate (S_{PT}) will decrease, if the average queue discharge headway *(h)* or the heavy-vehicle percentage of left-turn flows *(H_L)* increases.

Note that the constant 2.0 in the term *(h - 2.0)* represents the average queue discharge headway obtained from field observations. Using *(h - 2.0)* instead of *h,* the specification implies that the protected left-turn saturation flow rate equals 1780 vehicles per hour, in case of *h = 2.0* seconds and *H_L = 0 %.*

However, a further investigation of the model's residual distribution, shown in Figure 4.5, reveals that it violates one of the basic regression assumptions for having uniforrnly distributed residuals. More specifically, the proposed model structure tends to overestimate the saturation flow rate at both ends and underestimate it in the median

$$S_{PT} = 1746 \cdot \left(\frac{h}{2.0}\right)^{-0.88} \cdot \left(1 + 0.01 \cdot H_L\right)^{-0.57}. \tag{3}$$

The proposed non-linear specification yields both anticipated signs for all parameters and satisfactory goodness of fit as well. In addition, its residual properties are consistent with all underlying assumptions of regression, as shown in Figure 4.6. Again, by using the terms $(h\ /\ 2.0)$ and $(1 + 0.01 \cdot H_L)$, the model implies that the protected saturation flow rate, S_{PT}, equals 1746 vehicles per hour, when $h = 2.0$ seconds and $H_L = 0$ %.

Note that the protected left-turn saturation flow rate is sensitive to driving
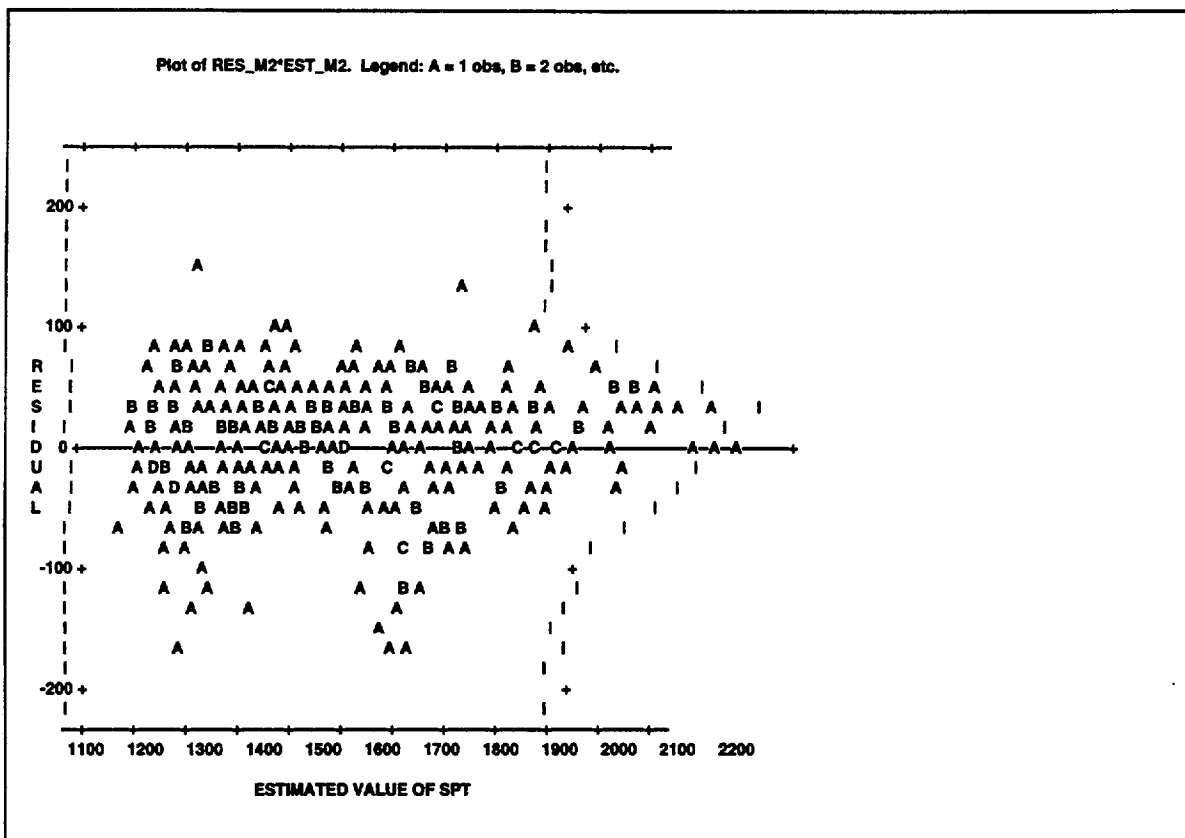

Figure 4.6 The plot of residuals versus estimated values for protected saturation flows from the revised (log-linear) model

respect to various sample sizes, the stability test has also been conducted and reported below.

Stability Test

The purpose of the stability test is to ensure that both the functional structure and estimated parameters will not vary with the use of different sample sets. A step-by-step description of the most commonly-used Chow statistic for such a purpose is presented below:

Step 1: Divide the entire data set into two subsets containing n_1 and n_2 observations, respectively.

Step 2: Estimate the proposed model of K parameters based on the entire (pooled) data set, and compute the unexplained variation (i.e. the error or residual sum of squares of the model):

$$\Sigma\, e_p^2 = \Sigma\, y_p^2 - \Sigma\, \hat{y}_p^2 \tag{4}$$

with $(n_1 + n_2 - K)$ degrees of freedom.

Step 3: Estimate the same model for each data subset, and compute the resulting unexplained variations:

$$\Sigma\, e_1^2 = \Sigma\, y_1^2 - \Sigma\, \hat{y}_1^2$$

$$\tag{5}$$

$$\Sigma\, e_2^2 = \Sigma\, y_2^2 - \Sigma\, \hat{y}_2^2$$

with $(n_1 - K)$ and $(n_2 - K)$ degrees of freedom, respectively.

Table 4.7 Summary of the stability test results for protected left-turn saturation flow rate

Basic Statistic	Pooled Data		First Subset		Second Subset	
No. Of Observations	300		150		150	
R^2 Value	0.9505		0.9527		0.9487	
Model SS (df)	6.8881	(2)	3.5451	(2)	3.3443	(2)
Error SS (df)	0.3585	(297)	0.1759	(147)	0.1810	(147)
Total SS (df)	7.2466	(299)	3.7210	(149)	3.5253	(149)
Variable	Parameter (t-Value)		Parameter (t-Value)		Parameter (t-Value)	
Intercept	7.4648	(1812.02)	7.4640	(1283.33)	7.4656	(1271.78)
$\ln(h/2.0)$	-0.8822	(-72.78)	-0.8930	(-52.42)	-0.8715	(-50.23)
$\ln(1+0.01 H_L)$	-0.5687	(-22.99)	-0.5696	(-16.35)	-0.5673	(-16.05)
Testing Statistic	Chow Test – Testing the stability of model parameters					
F^* Statistic	0.4228					
$F_{.05, v1, v2}$	2.6353					
$H_0: b_1 = b_2$	Accept					

Table 4.7 shows the summarized statistics and the testing results of the revised (log-linear) model. Notably, the statistic F* of the model is less than the critical value $F_{0.05}$, v1 v2, and one can thus conclude that both the model structure and parameters have no significant difference between the first and the second data subsets, and the developed model can be employed in practice.

All selected field sites share the following common features:

- Protected phase with one exclusive left-turn lane;

- Left-turn flows cannot be completely discharged during each cycle in the

  observed peak period;

- Drivers have been observed to consistently use the amber phase for left-

  turns; and

- Drivers are relatively conservative and exhibit an average discharge headway

  of longer than 2 seconds.

With the information in Table 4.8, we have employed the following two equations to

compute the resulting left-turn capacity for each field site:

HCM Method:

$$\text{LT Capacity} = 1900 \text{ vphpl} \times 0.95 \times (\text{truck adjustment factor}) \cdot \left(\frac{\text{Ge} + \text{amber}}{\text{cycle length}} \right)$$

Our Proposed Method:

$$\text{LT Capacity} = 1746 \text{ vphpl} \cdot \left(\frac{\text{Ave. D}}{2.0} \right)^{-0.88} \cdot (1 + \text{truck percentage})^{-0.57} \cdot \left(\frac{\text{Ge} + \text{amber}}{\text{cycle length}} \right)$$

The estimation results with these two methods along with measured field capacity for

each site are summarized below:

Site	HCM	U of M	Measured Capacity
1	383 vph	361 vph	370 vph
2	383	353	364
3	394	358	340
4	343	310	300
5	306	299	281

References:

[1] Teply, S (1984), "Canadian Capacity Guide for Signalized Intersections: An Overview", Transportation Research Record 1320.

[2] Teply, S. and Jones, A. M. (1991), "Saturation Flow: Do we speak the same language?', Transportation Research Record 1320.

[3] Akcelik, R. (1989), "Traffic Signal: Capacity and Timing Analysis", Research report ARR No. 123. Australian Road Research Board.

Chapter 5: Queue Length Prediction Model

5.1   Introduction

Queuing process is an important subject in traffic engineering, since various traffic

problems are related to queuing conditions in a network system For instance, in the analysis of

left-turn capacity, queue information is essential to determine the effective green for permitted

left-turns and to analyze the blockage conditions of left-turn bays.   The purpose of this chapter is

to construct a model with a calibrated simulation program (i.e., TRAF-NETSIM), which can

estimate the maximum number of queued vehicles among these "target through" lanes at the

beginning of a green phase.

The chapter is organized as follows. Section 5.2, presents a general discussion about

these factors associated with the intersection queuing length. Section 5.3 illustrates the

experimental design with respect to the acquisition of essential simulation data for model

development. Section 5.4 highlights the core modeling concept, including the stability test and

performance evaluation. Section 5.5 summarizes research findings as well as further

enhancements.

5.2   Factors Contributing to Intersection Queue Length

Theoretically, a queuing process is determined by the interactions between demand-side

(arrival rate) and supply-side (service rate) patterns. The queuing size increases when the arrival

rate is larger than the service rate, but decreases when the service rate is larger than the arrival

rate. In traffic studies, the queuing conditions of a given movement can be analyzed through its

calibrating simulation parameters from field data have been presented previously in Chapter 2.

Network Design

As illustrated in Figure 5.1, a two-intersection network system is employed for use in simulation experiments. In order to realistically simulate the arrival and discharge flow patterns for queuing estimation, both intersections are given with signal control. Basically, the function of the upstream signal is to generate a relatively reasonable flow pattern filtered through a signalized intersection. In contrast, the downstream signal is to regulate the discharging flow based on its signal phasing and timing.

Besides, the geometric conditions, including the number of lane(s) on the target link and the link-length between upstream and downstream intersections, are factors contributing to the formation of queue, and thus have been considered in the design of simulation experiments. As for traffic flow conditions, in addition to the volume on the target link, the experimental scenarios take into account the impacts due to variations of the desired speed (or posted speed limit) and the heavy-vehicle percentage in the flow. The impacts of signal phasings, settings, and offsets between upstream and downstream intersections have also been included in the experimental design.

For convenience of experimental design but without loss of the key functions, we have made some assumptions. First, the flow rate is so preset that through traffic from the main link, rather than the side streets will dominate the development of through queue at the target link. Secondly, the signals at both intersections are assumed to be pretimed, sharing a common cycle length, as signal coordination has been taken into account. Third, only through movements have been considered in the target link since our primary interested lies in the through queuing

interactions with other factors. Also, from the perspective of through vehicles, the only two

phases they would experience are green and red durations.

<u>Definition of Variables</u>

The definition of variables used in the simulation experiments is presented below:

Variables	Unit	Definition
N	Lane	Number of lanes for through traffic on the target link;
L	ft	Length of the target link;
F_i	vph	Total input (through) flow rate to the target link;
V_o	mph	Desired speed (or posted speed limit) on the target link;
H_0	%	Heavy-vehicle percentage on the target link;
C	sec	Signal cycle length for both intersections;
G_U	sec	Green duration at the upstream intersection;
R_U	sec	Red duration at the upstream intersection;
G_D	sec	Green duration at downstream intersection;
R_D	sec	Red time at the downstream intersection;
$(G/C)_U$		G/C ratio for the upstream signal, i.e., G_U / C;
$(G/C)_D$		G/C ratio for the downstream signal, i.e., G_D / C;
O	sec	Signal offset computed for the beginning of green phase at the downstream intersection

Table 5.1. Variables in Simulation Experiments for Queue Model

Independent Variable	Unit	Lower Bound	Upper Bound	Increment
N	lane	1	4	1
L	ft	500	4000	500
F_I	vph	100	*1	100
V_O	mph	25	55	5
H_O	%	0	30	3
C	sec	50	160	10
$(G/C)_U$		0.3	0.7	0.1
$(G/C)_D$		0.3	0.7	0.1
O	sec	0	*2	10

Dependent Variable	Relationship
$G_U{}^3$	$C * (G/C)_U$
$R_U{}^3$	$C - G_U$
$G_D{}^3$	$C * (G/C)_D$
$R_D{}^3$	$C - G_D$

Note: 1. The upper bound of F, = MIN($N*3600*(G/C)_U/2.5$, $N*3600*(G/C)_D/2.5$).
        2. The upper bound of 0 = C - 10.
        3. $0 < G_U$, R_U, G_D, and $R_D < 120$.

five different states. The estimated log-linear model is given below:

$$\ln Q_M = 0.8407 \cdot \ln Q + 0.2140 \cdot \ln N - 0.1957 \cdot \ln C + 0.8691 \cdot \ln (G/C)_U$$
$$\quad\quad (17.69) \quad\quad\quad (4.64) \quad\quad\quad (6.15) \quad\quad\quad (9.96)$$

$$+ 0.3376 \cdot \delta \cdot \ln P_p + 0.3849 \cdot (1-\delta) \cdot \ln P_N$$
$$\quad (12.38) \quad\quad\quad\quad (14.57)$$

$R^2 = 0.9556,$ No. of Cases = 273

(1)

$$Q_M = Q^{0.8407} \cdot N^{0.2140} \cdot C^{-0.1957} \cdot (g/c)_U^{0.8691} \cdot P_P^{0.3376 \cdot \delta} \cdot P_N^{0.3849 \cdot (\delta-1)}$$

(2)

where:

Q equal to $(F_P / (G/C)_U \cdot (R_D / 3600)$, (veh);

F_P equal to F_o / N, and represents the per-lane (through) flow rate approaching the target

intersection during each hour (vphpl);

P_P equal to $T_T - O$ (if $T_T - O > 0$), or 1 (otherwise), and represents the signal progression

factor, (second);

P_N equal to $O - T_T$ (if $T_T - O < 0$), or 1 (otherwise), and represents the signal progression

factor, (second);

T_T equal to MOD $(L/(0.8 \cdot V_o \cdot (5280/3600))$, C), and C is the cycle length;

δ is a binary variable, and equals to 1 (if $T_T - O > 0$), or 0 (otherwise);

O offset of the green phase between two neighboring intersections;

Note that although there is only the F_P flow rate moving toward the target intersection, all

those vehicles are coming in platoons only during the green phase of the upstream signal. As

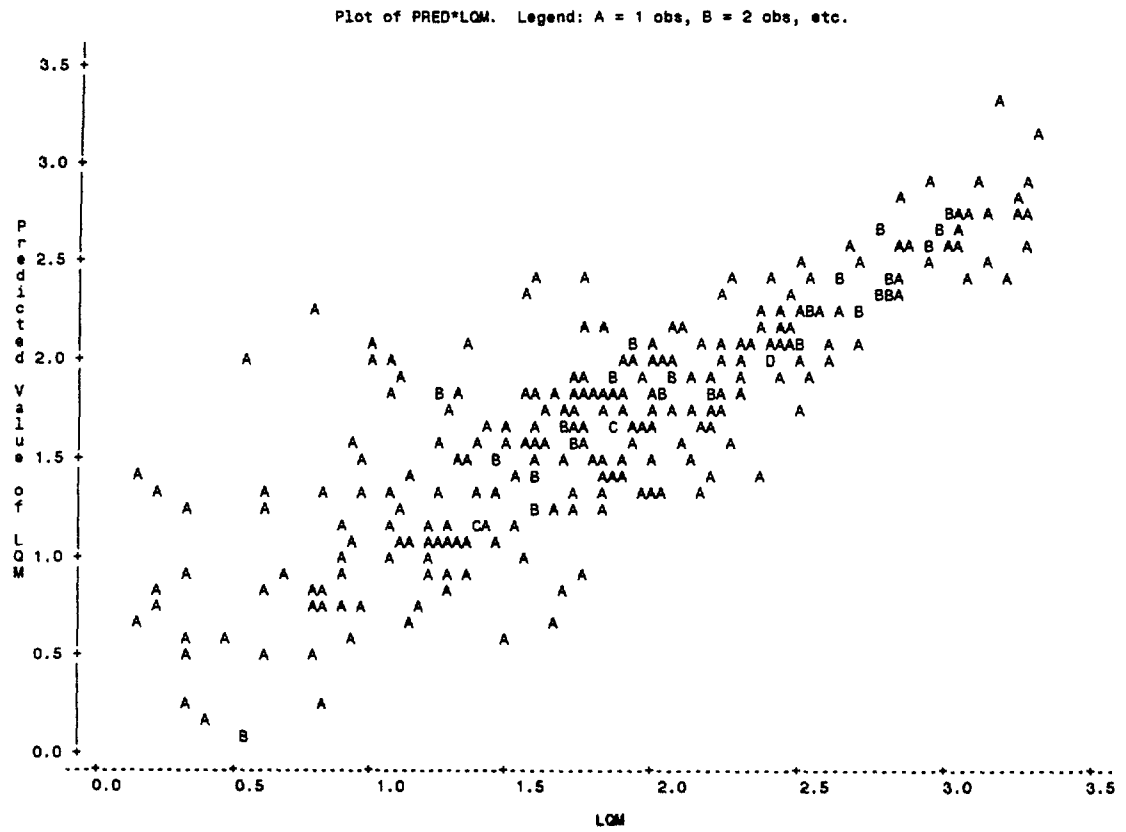such, the equivalent flow rate that contributes the development of the queue is actually

Figure 5.2. Scatterplot of Observed v.s. Estimated Values for the Proposed Queue Model

Table 5.2 Stability Test for Queue Model

Queue Model								
$Q_M = Q^a \cdot N^b \cdot C^c \cdot (G/C)_U^d \cdot P_P^{e \cdot \delta} \cdot P_N^{f \cdot (1-\delta)}$								
Data Set	Obs. No.	R^2	a	b	c	d	e	f
Whole	273	0.9556	0.8407 (17.69)	0.2140 (4.64)	-0.1957 (6.15)	0.8691 (9.96)	0.3376 (12.38)	0.3849 (14.57)
1st Half	141	0.9455	0.8384 (10.70)	0.1977 (2.67)	-0.2099 (3.73)	0.9132 (6.76)	0.3570 (8.11)	0.4155 (9.62)
2nd Half	132	0.9676	0.8418 (14.66)	0.2332 (4.09)	-0.1840 (5.13)	0.8404 (7.62)	0.3257 (9.64)	0.3602 (11.22)

Note: 1. $Q = (F_P/(G/C)_U) \cdot (R_D/3600)$.
2. Unexplained variations: $\sum e^2_{1+2} = 42.39$, $\sum e^2_1 = 26.99$, and $\sum e^2_2 = 14.91$.
3. $F^* = 0.52$.

Table 5.3 Estimation Results for Queue Model

OBS	N	L	FO	VO	VL	HO	HL	GD	RD	GU	RU	C	O	QM	QMO	DMO	PMO
1	1	3500	304	40	30	27	9	25	65	35	55	90	70	3.1	2.82	-0.27	-0.08
2	4	3000	1800	55	35	3	21	65	95	65	95	160	60	2.9	10.59	7.69	2.65
3	1	3500	399	55	35	21	24	50	20	40	30	70	60	0.5	1.64	1.14	2.28
4	2	500	798	45	35	21	27	90	40	40	90	130	0	0.0	3.23	3.23	.
5	1	1000	198	25	35	18	3	20	50	50	20	70	50	2.4	2.92	0.52	0.22
6	1	500	698	25	50	9	6	30	20	35	15	50	40	7.6	4.80	-2.79	-0.36
7	3	2500	299	40	55	30	21	55	85	85	55	140	10	2.8	3.47	0.67	0.24
8	2	3000	100	40	30	24	12	70	50	50	70	120	60	0.4	0.51	0.11	0.29
9	1	3500	602	35	55	6	24	80	80	95	65	160	30	19.1	12.51	-6.58	-0.34
10	4	2000	1904	45	25	15	21	50	70	50	70	120	90	17.9	15.29	-2.60	-0.14
11	1	2500	199	45	50	0	0	60	40	40	60	100	30	0.0	2.02	2.02	.
12	2	4000	501	55	40	18	6	30	20	30	20	50	30	2.5	2.13	-0.36	-0.14
13	1	4000	198	50	35	18	15	20	50	20	50	70	60	1.6	1.99	0.39	0.24
14	3	3500	300	30	35	30	0	50	50	50	50	100	10	2.5	3.02	0.52	0.21
15	3	4000	1497	55	45	9	30	50	50	70	30	100	50	4.4	5.98	1.58	0.36
16	1	500	100	30	40	30	18	55	85	100	40	140	100	3.4	4.30	0.90	0.26
17	3	1000	594	45	35	21	27	30	30	25	35	60	0	2.5	2.27	-0.22	-0.08
18	4	3000	903	55	40	15	30	35	35	50	20	70	10	4.6	3.78	-0.81	-0.17
19	3	3000	301	25	35	18	3	95	65	65	95	160	30	1.5	3.19	1.69	1.12
20	2	2500	396	35	55	9	27	30	20	15	35	50	40	1.2	2.06	0.86	0.72
21	3	1500	2901	40	30	0	6	70	30	70	30	100	60	10.5	10.60	0.10	0.00
22	2	1000	600	40	30	9	9	50	70	60	60	120	20	1.1	2.14	1.04	0.95
23	1	3500	804	40	40	6	15	100	40	85	55	140	120	14.7	10.26	-4.43	-0.30
24	1	3500	298	30	40	24	12	45	45	55	35	90	0	1.1	2.63	1.53	1.39
25	1	4000	297	30	45	0	0	40	60	50	50	100	70	6.3	7.21	0.91	0.14
26	3	2500	201	25	40	21	3	70	50	70	50	120	30	1.6	1.78	0.18	0.11
27	2	4000	600	40	40	0	21	65	25	45	45	90	50	1.0	2.90	1.90	1.90
28	2	3500	301	50	30	30	24	50	50	60	40	100	0	4.0	3.43	-0.56	-0.14
29	1	2500	496	25	40	27	0	30	20	30	20	50	30	1.7	1.87	0.17	0.10
30	3	4000	1101	50	50	21	3	60	60	50	70	120	110	12.9	9.32	-3.57	-0.27
31	2	500	502	35	45	24	0	70	70	40	100	140	90	9.5	8.62	-0.87	-0.09
32	1	1000	798	40	40	24	24	85	55	100	40	140	100	20.6	16.54	-4.05	-0.19
33	2	3000	803	45	45	3	24	100	40	100	40	140	90	8.8	5.91	-2.88	-0.32
34	3	1000	499	45	40	12	21	65	95	50	110	160	80	8.3	7.65	-0.64	-0.07
35	4	1000	297	55	30	21	0	30	20	20	30	50	40	2.0	0.99	-1.00	-0.50
36	1	2000	300	40	35	6	21	45	105	60	90	150	120	12.5	12.07	-0.42	-0.03
37	3	1500	1798	50	25	24	15	65	25	45	45	90	20	0.0	3.04	3.04	.
38	4	1000	899	50	55	15	6	90	40	50	80	130	80	3.4	5.36	1.96	0.57
39	1	2500	199	35	45	24	12	40	90	65	65	130	110	6.9	6.52	-0.37	-0.05
40	4	2500	600	50	35	27	27	50	50	60	40	100	80	4.5	4.02	-0.47	-0.10
41	1	3000	199	50	40	30	21	70	70	85	55	140	20	2.2	3.73	1.53	0.69
42	1	500	299	35	55	24	12	40	100	40	100	140	70	11.7	10.36	-1.33	-0.11
43	1	1000	497	55	30	15	21	35	55	35	55	90	80	12.2	11.03	-1.16	-0.09
44	2	4000	700	35	30	12	6	65	95	50	110	160	150	16.6	12.38	-4.21	-0.25
45	4	4000	1195	40	50	6	3	25	25	35	15	50	10	3.1	3.40	0.30	0.09
46	3	3000	697	40	45	21	6	40	100	100	40	140	90	7.3	8.01	0.71	0.09
47	1	3000	300	45	30	9	30	25	65	35	55	90	20	7.5	5.64	-1.85	-0.24

QMO: the estimated queue length
DMO: the difference
PMO: the percentage difference

Chapter 6: The Effects of Bay Length on Left-turn Capacity

6.1 Introduction

The analysis of left-turn capacity under various left-turn bay lengths is a quite complex task. It has not been addressed in the current HCM procedures. As with a given bay length, the left-turn capacity depends not only on its own "supply" and "demand" levels, but also several other factors, such as the through queue length. In principle, the left-turn bay can be viewed as a left-turn lane if it is longer than the required length. Otherwise, when the bay length is relatively short, or the through flow rate is relatively high, some left-turn vehicles may be blocked by the through queue (see Figure 6.1). Consequently, the green phase for the left-turn vehicles may not be fully utilized, and the actually usable left-turn capacity will be thus lower than that estimated primarily with G/C ratios and saturation flows.

To account for the bay-length effect is thus an essential task for reliable estimation of left-turn capacity. Conceivably, the first step to formulate the bay-length impact on capacity is to understand the complex interactions between all associated factors. For instance, the through flow rate and signal settings may affect the maximum through queue size, and thus have impacts on the left-turn capacity. The left-turn flow rate may also have impact on the fraction of left-turn phase during which the through queue length may have exceeded the left-turn bay. Moreover, in a signalized urban network where vehicles mostly arrive in platoons, such relations become intractable, as the distribution of platoon starting times and size may also have significant effects on the left-turn capacity.

In view of the critical role of the bay length on left-turn capacity, this chapter intends to

analyze its interrelations with key associated factors, including signal settings and through flow rates, The purpose of this study is to develop a model for estimation of unusable left-turn green duration due to insufficient bay length. To take advantage of some trackable relations, but also encompass all complex interactions, this study has employed a two-stage analysis method. The core of stage I is to derive analytical relations with the existing queuing theory and some simplified assumptions, while the primary work of stage II is to include all intractable interactions through simulation experiments. This final product is a hybrid model that consists of both an analytical formulation and adjustment terms calibrated from regression analysis.

There are two primary scenarios in the analytical analysis. Scenario I considers a base case in which the arrival rates are assumed to be constant. The results of Scenario I have been extended in the second scenario to account for the platoon impacts on the arrival patterns, and on the blocked portion of left-turn green phase.

The remaining sections are organized as follows. Section 2 presents a theoretical model with a uniform arrival assumption. Section 3 highlights an enhanced formulation under the platoon arrival patterns. Section 4 describes the core concept as well as experimental procedures for developing a hybrid empirical model under various traffic conditions. Last section summarizes the concluding comments and further research needs.

6.2 Base Model--Uniform arrival patterns

To facilitate the analysis, Scenario I starts with the assumption of having uniform arrivals for both left-turning and through flows under a protected signal phasing. All variables involved in the following analysis are defined below:
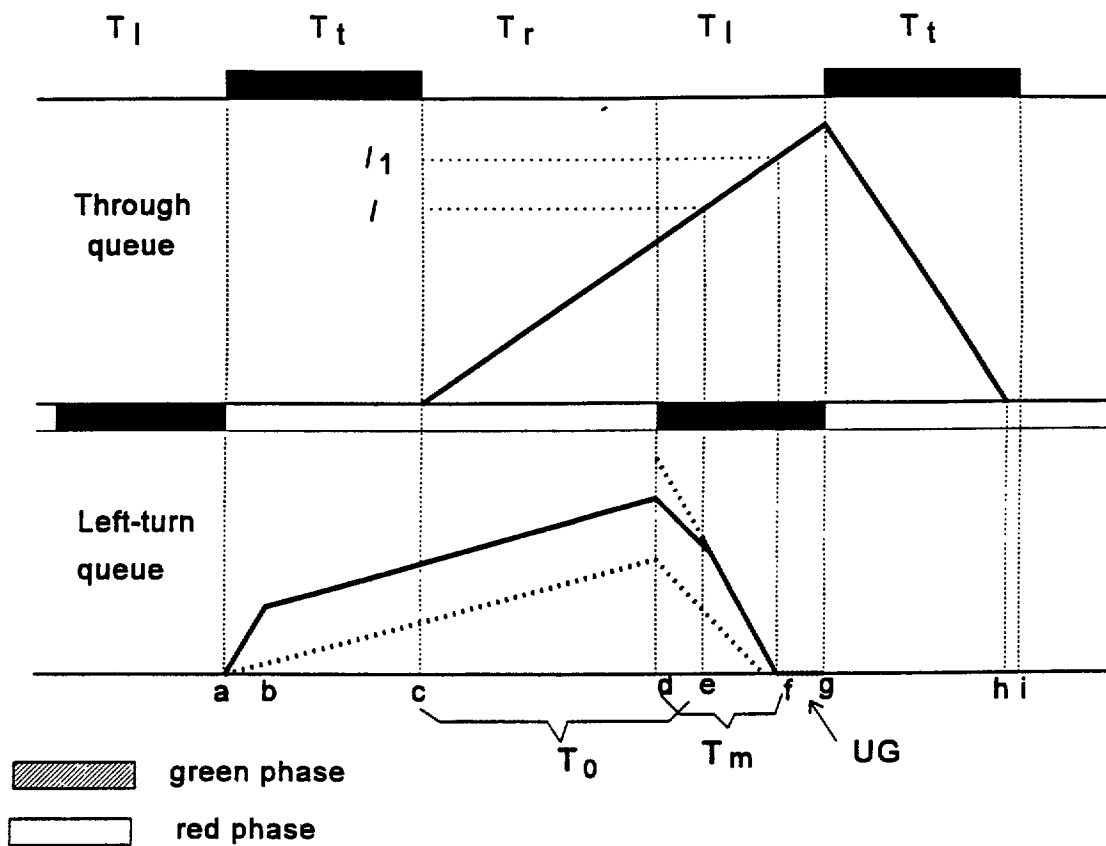
Figure 6.2 A graphical illustration of the interrelation between *UG* and the bay length under the condition of uniform arrivals and $T_0 > T_r$

$$l_1 = (T_r + T_m) r_l a \qquad (2)$$

With respect to the critical value l_0, there are three cases to be investigated.

Case 1: $T_r r_t \geq (T_r + T_l + T_t) r_l$, then $l_0 = (T_r + T_l + T_t) r_l a$.

Under such a case, one can easily conclude that $T_r r_t a \geq l_0$. It implies that if the bay length is set to l_0, the blockage will begin during the red phase for left-turn, as illustrated in Figure 6.3. In such a case, the maximum left-turn queue length is

$$Q_{max} = (T_t + T_r + T_l) r_l a = l_0 \qquad (3)$$

Case 2: $(T_t + T_r) r_l - T_l r_t < T_r r_t < (T_r + T_l + T_t) r_l$, then $l_0 = [(T_l + T_r + T_t) r_l + T_r r_t] a / (1 + r_l / r_t)$.

If the bay length is set to l_0, then T_0, the duration from the beginning of a through red phase to the start of the blockage, is $l_0 / (r_t a)$. Under the condition that $T_r r < (T + T + T) r$, one can easily conclude that $T_r r_t a < l_0$. It indicates that the blockage will begin during the green phase for left-turn. As illustrated in Figure 6.2, the left-turn queue will reach its maximum at the beginning of the left-turn phase. One can approximate such a length with the following expression:

$$Q_{max} = (T_t + T_r) r_l a + (T_r + T_l - T_0) r_l a \qquad (4)$$

where the first term consists of left-turn vehicles arriving during the red phase, while the second term captures those being blocked in the previous cycle, but arriving during the current cycle. By replacing T_0 in Eqn (4) with $l_0 / (r_t a)$, Eqn (4) can be restated as:

$$Q_{max} = (T_t + T_r) r_l a + (T_r r_t + T_l r_t - T_r r_l - T_t r_l) a r_l / (r_t + r_l)$$
$$= [(T_l + T_r + T_t) r_l + T_r r_t] a / (1 + r_l / r_t) = l_0 \qquad (5)$$
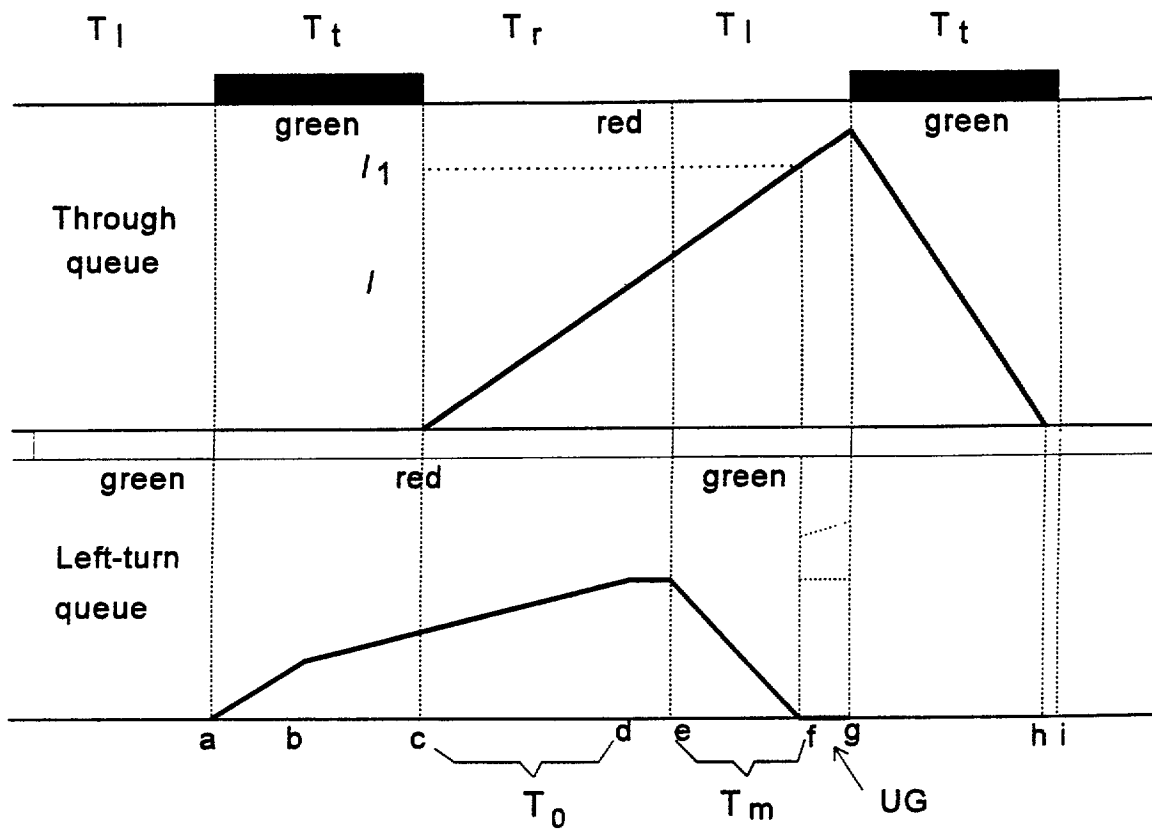
Figure 6.3 A graphical illustration of the interrelation between *UG* and the bay length under the condition of uniform arrivals if $T_0 \le T_r$

$(T_r+T_l)r_l a$ (see Figures 6.4 and 6.5). In such a case, the entire green phase for left-turn vehicles is usable.

- $UG=T_l+T_r-l/(r_l a)$ if the bay length l is shorter than $(T_l+T_r)r a$, but longer than $max(l_0, l_1)$ (see Figures 6.4 and 6.5). The left-turn queue in the bay should have been cleared by the onset of blockage due to through queue. All green time after the blockage is unusable.

- $UG=T_l-T_m$ if the bay length l is shorter than $max(l_0, l_1)$ but longer than l_0 (see Figure 6.4). The green time after the discharge of left-turn queue will be unusable.

Note that if the bay length l is shorter than l_0, the maximum left-turn queue will be longer than the bay length. Their interrelations under such a case is quite complex as UG depends on the distribution of left-turn and through vehicles in the queue beyond the left-turn bay. As a result, UG will vary between (T_l-T_m) and $(T_l-l/(r_d a))$. One may conveniently set UG to (T_l-T_m) when $l < l_0$ for conservative estimation of left-turn capacity.

6.3 An Extended Model for Platoon Arrivals

Note that the above base case may provide a reasonable approximation for use at isolated congested intersections. It certainly does not consider the interactions between neighboring intersections in which vehicles may arrive in platoons due to the signal control effects. Hence, in the following analysis, the computation of unavailable green phase for left turn will take in into account of non-uniform arrival patterns. For convenience of analysis, the entire cycle is divided into two intervals with respect to the arriving flow patterns, i.e., platooning arrivals and constant arrivals. Additional variables involved in the hereafter analysis are defined below:
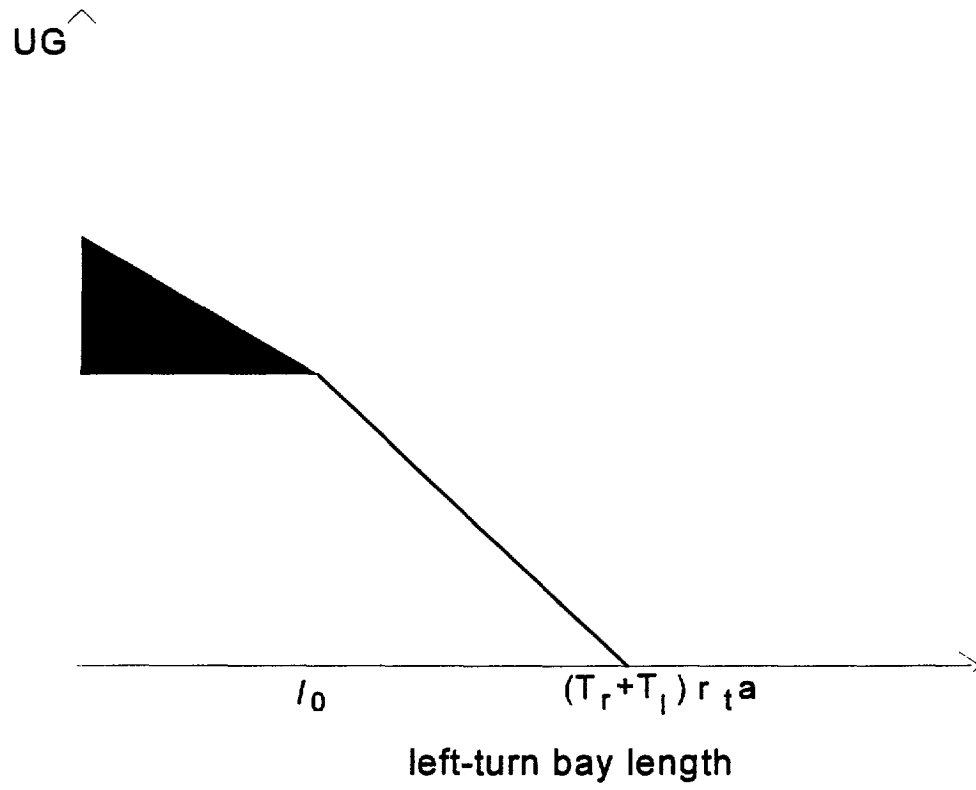
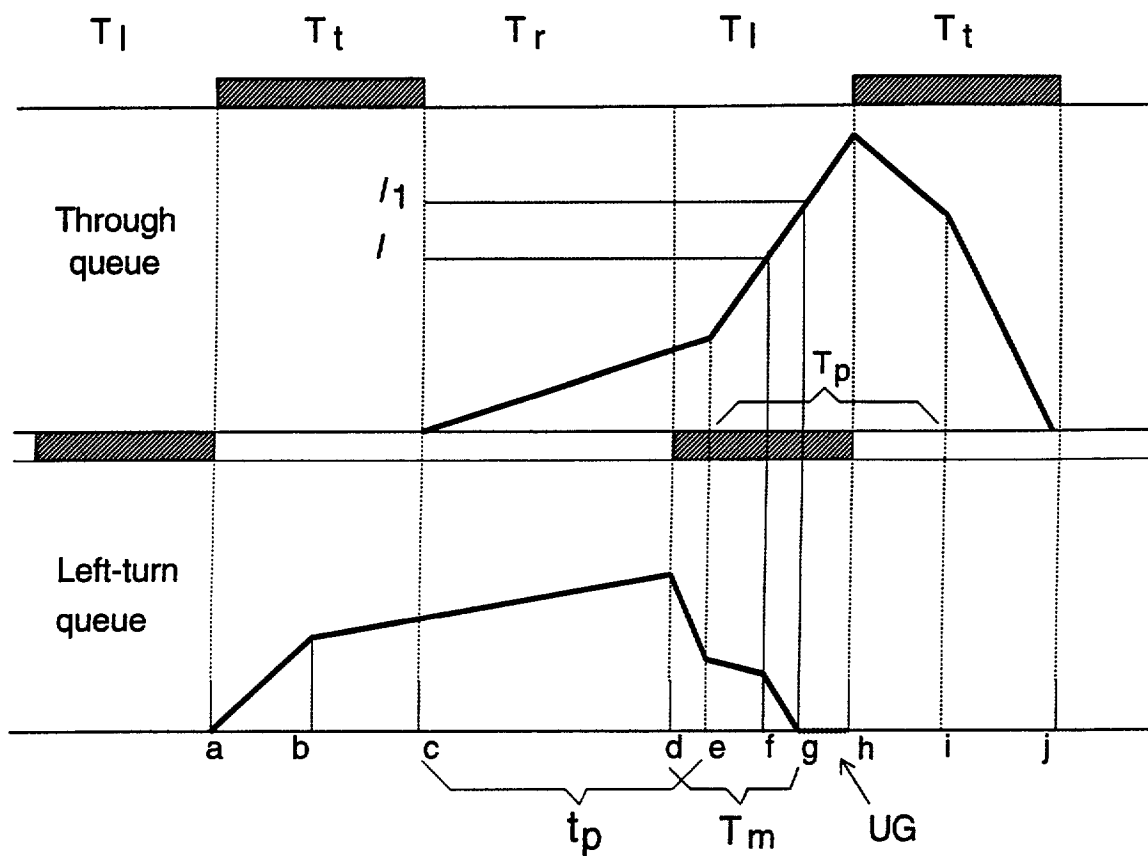**Figure 6.5** The relation between *UP* and the bay length if $l_0 \geq l_1$

Figure **6.6**   A graphical illustration of the interrelation between *UG* and the bay length under mixed arrival patterns (platoons arrive during the red phase for through vehicles)

shall have been discharged by the time the through queue has exceeded the bay length. Otherwise, some left-turn vehicles may remain in the bay.

The analytical derivations of the above conclusions are reported below.

For the first statement, one shall consider the following four cases:

Case 1: $L \leq T_r r_{to} a$, then $l_0 = L$.

Clearly, if the bay length is set to equal l_0, the blockage shall take place during the red phase for left-turns, and the maximum left-turn queue length is thus

$$Q_{max} = [(T_l + T_r + T_l - T_p) r_{lo} + T_p r_{lp}] a = L = l_0 \qquad (14)$$

Case 2: $T_r r_{to} a < L < t_p r_{to} a + (t_p - T_r) r_{lo} a$

Under such a case, l_0 is equal to:

$$l_0 = (L + T_r r_{lo} a)/(1 + r_{lo}/r_{to}) \qquad (15)$$

From the relation, $T_r r_{to} a < L < t_p r_{to} a + (t_p - T_r) r_{lo} a$, it leads to the following inequality:

$$T_r < \frac{l_0}{r_{to} a} < t_p \qquad (16)$$

If the bay length is set to equal l_0, the inequality (16) implies that the blockage due to through queue should take place during the left-turn green phase but in the non-platooning period. Hence, the maximum left-turn queue length can be approximated:

$$Q_{max} = L - (\frac{l_0}{r_{to} a} - T_r) r_{lo} a \qquad (17)$$

If the bay length is set to equal l_0, the left-side term of the above inequality is actually the maximum through queue length, while the right-side term is the bay length. Inequality (22) implies that the maximum through queue should not exceed the bay length if it is set to equal l_0. Hence, the maximum left-turn queue length is equal to:

$$Q_{max} = L - (t_p - T_r) r_{lo} a - (T_r + T_l - t_p) r_{lp} = l_0 \tag{23}$$

As for the second statement, one shall consider the following two cases: (1) $t_p > T_r + T_m$; (2) $t_p \leq T_r + T_m$.

Case 1: $T_r + T_m < t_p$, then $l_1 = (T_r + T_m) r_l a$.

If left-turn bay length l equals to l_1, the blockage due to through queue should take place during the left-turn green phase, and T_0, the time duration from the beginning of a through red phase to the start of the blockage, is equal to $T_r + T_m$. Thus, the maximum left-turn queue length is

$$Q_{max} = L - T_m r_{lo} a \tag{24}$$

· The duration to completely discharge such a queue length is thus:

$$(L - T_m r_{lo} a)/(r_d - r_{lo}) = T_m \tag{25}$$

Eqn (25) implies that all vehicles in the left-turn queue should have been discharged prior to the onset of blockage.

Case 2: $t_p \leq T_r + T_m$, then $l_1 = t_p r_{to} + (T_r + T_m - t_p) r_{tp}$.

If the bay length l is set to equal l_1, then T_0 (the time duration from the beginning of a through red phase to the start of the blockage) shall be computed as follows:

$$Q_r = Q_{max} - (T_0 - T_r)(r_d - r_{lo})a$$
$$= L - (T_0 - T_r)r_d a \tag{29}$$

The additional time period needed to completely discharge the remaining left-turn queue is $(L/(r_d a) - T_0 + T_r)$. Thus, the total time required to discharge the entire left-turn queue is $(L/(r_d a) + T_r)$, and consequently, the unusable green phase, UG, is equal to

$$UG = T_r + T_l - (\frac{L}{r_d a} + T_r) = T_l - T_m \tag{30}$$

Case 2: $t_p < T_0$ - Platoons arrive prior to the blockage

The resulting maximum left-turn queue length should be equal to

$$Q_{max} = L - (T_0 - T_r)r_{lo}a - (t_p - T_0)r_{lp}a \tag{31}$$

By the onset of bay blockage, the remaining left-turn queue length, Q_r, is

$$Q_r = L - (T_0 - T_r)r_{lo}a - (t_p - T_0)r_{lp}a - (T_0 - T_r)a(r_d - r_{lo}) - (t_p - T_0)$$
$$= L - (T_0 - T_r)r_d a \tag{32}$$

The additional time required to discharge the remaining queue is $(L/(r_d a) - T_0 + T_r)$. Thus, the unusable green phase, UG, is

$$UG = T_r + T_l - (\frac{L}{r_d a} + T_r) = T_l - T_m \tag{33}$$

If the bay length is longer than l_1, it leads to the following relation: $T_0 > T_r + T_m$. Under such a condition, no left-turn queue may exist in the bay by the onset of blockage. Hence, the resulting unusable green phase, UG, equals the time duration from the beginning of blockage to the end of
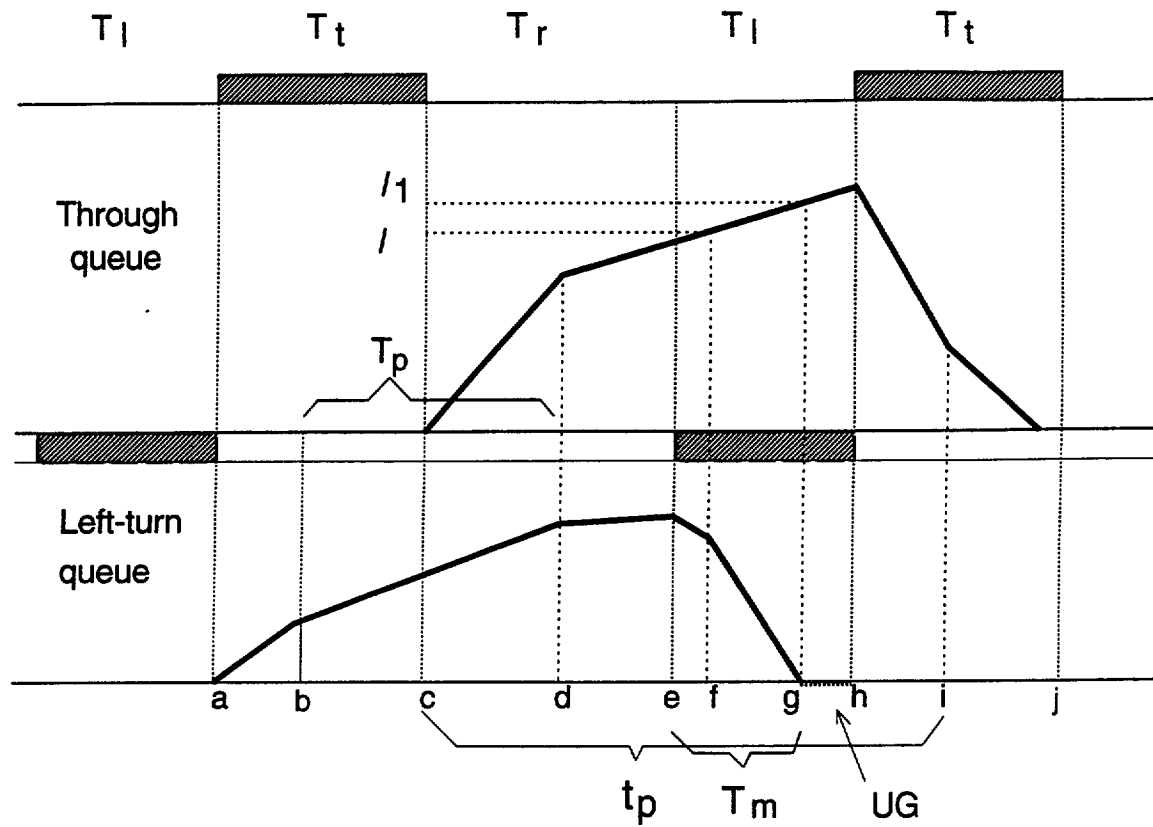
Figure 6.7 A graphical illustration of the interrelation between *UG* and the bay length when platoons arrive during the green phase for through vehicles

allow to investigate other possible contributing factors. The experimental design as well as estimation results are summarized below:

<u>Simulation Experiments:</u>

Table 6.4 presents all variables involved in the design of simulation experiments, including their ranges of variation. The entire set of experiments consists of 300 simulation scenarios generated with a random sampling strategy. Figure 6.8 illustrates the example network used to simulate those sampled traffic scenarios. Similar to all previous analyses, we have employed the most reliable network simulation program to date, TRAF-NETS&l, as the prime tool, and collect each potential contributing variable as well as the actual unusable green duration from the outcome of an 1.5 hour simulation. To minimize the stochastic variation due to the complex traffic nature, we have conducted five replications for each simulation case and take the average for use in the statistical model estimation.

Note that to collect all necessary data at the desired level of accuracy we have placed detector at a spacing of 20 feet along the entire left-turn bay and its neighboring through lane. The resulting queue length as well as flow rates were collected at an interval of 3 seconds.

<u>Model Estimation</u>:

The estimation of a hybrid regression model for unusable green time was based on standard procedures, including an exploratory analysis, selection of primary factors with t-statistics, the evaluation of estimated parameter signs, the model stability under different samples, and the resulting goodness of it. Eqn (36) presents the final investigation results which intend to minimize the number of variables needed for estimation but without loss of the key underlying relations.
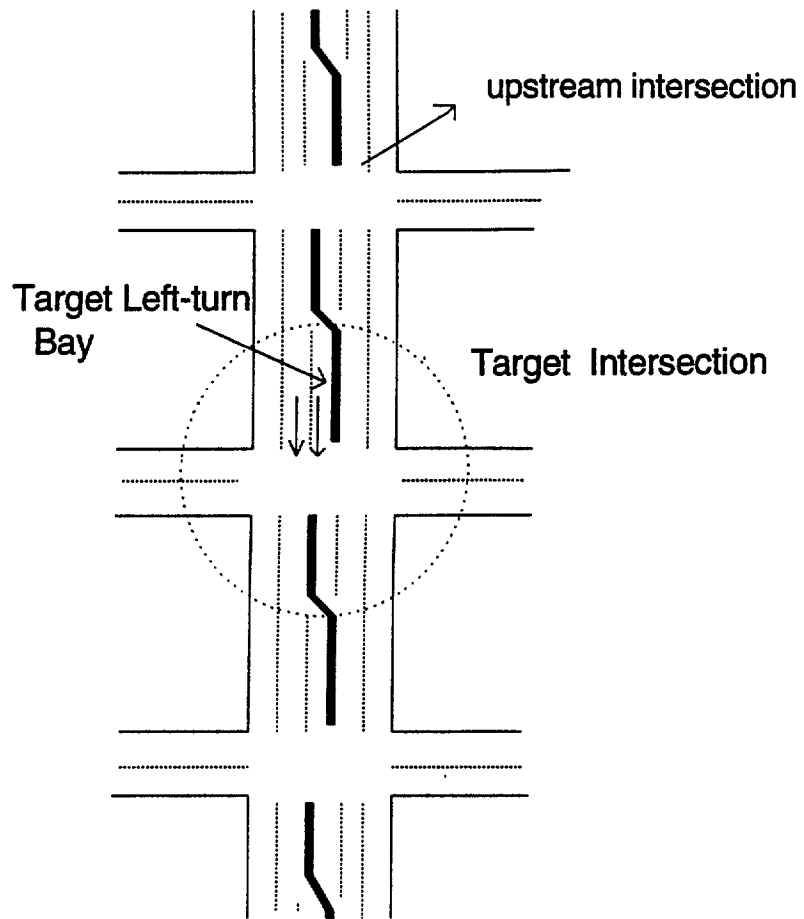
Figure 6.8   A graphical illustration of the example road network used in the simulation experiment

setting on the unusable green duration.

The entire data set for model calibration consists of 300 different simulated systems. Figure 6.9 presents the comparison results between the estimated and simulated unusable green fractions under various simulated cases. Considering the complexities of such a highly stochastic issue, one shall be comfortable with the achieved results.

<u>Summary of Application Procedures</u>

To facilitate the application of the bay length impact model, we have summarized these key steps and input variables below:

Step 1:   *Compute the information **for** the following variables:*

r_t: average through flow rate per lane

r_l: average left-turn flow rate per lane

$(G/C)_l$:   green time/cycle time for left-turn movement

$(G/C)_t$:   green time/cycle time for through movement

$(G/C)_{t'}$:   green time/cycle time for through movement at the upstream intersection

UGE: an analytical term for the unusable fraction of left-turn green duration that should be estimated with the following expressions:

I: the left-turn bay length

T_l: green duration for left-turn movement per cycle

T_t: green duration for through movement per cycle

T_r: red duration for both through and left-turn vehicles per cycle

r_l: left-turn arriving flow rate (VPH)

r_d: saturation discharging rate for left-turn flows (VPH)

6-29

signal settings with the following equation:

$$UFG = 0.58 \, UGE + 0.36 \times 10^{-3} \cdot \frac{r_l}{(G/C)_u}(1-(G/C)_l)-0.67 \times 10^{-3}\frac{r_l}{(G/C)_u}+0.55 \, (G/C)_l$$

Where UGE = UG/T_l

Step 4:   *Adjust the left-turn capacity due to an insufficient bay length with the following expression:*

$$C_{LT}^* = C_{LT} \cdot (1 - UFG)$$

Where C_{LT} and C_{LT}^* are the initial and adjusted left-turn capacities, respectively.

6.5 Closure

The critical impact of bay length and left-turn capacity has long been recognized, but yet not adequately addressed in the existing traffic literature due to the complex interactions among all associated factors. This study has started with an analytical derivation of the interrelations between unusable left-turn green duration due to through queue blockage, and the bay length as well as arriving flow rates. A set of relations has been generated for use under congested isolated intersection. To account for the signal coordination condition, we have extended the model to incorporate the scenarios which contains both platoon and non-platoon arriving patterns due to the upstream signal control.

As analytical models often suffer from the use of assumptions which may not always in consistence with some traffic conditions, we have developed a set of complementary components, based on the results of extensive simulation experiments. The proposed hybrid model, including the analytical term and all complementary components along with their parameters from regression analysis, offers a convenient and effective tool for bay length impact assessment. Given the unusable
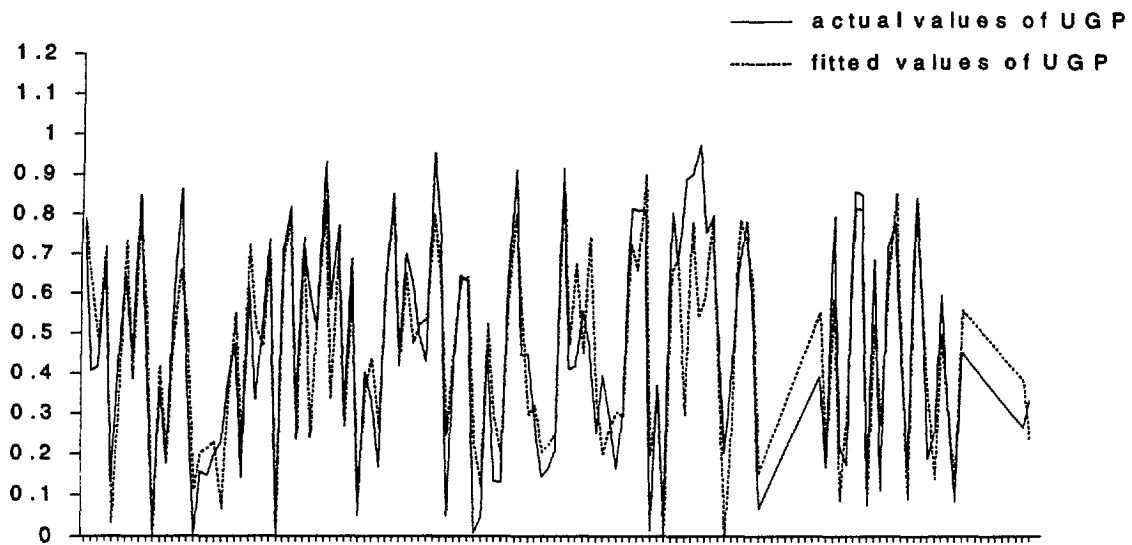
Figure 6.9(b). Comparison between actual values and fitted values of *UPG* (cases 101-200)

Chapter 7: Procedures for Exclusive Left-turn Capacity Analysis

7.1 Introduction

This chapter provides a detailed description of procedures for analysis of exclusive left-turn capacity under protected, permitted, protected/permitted, and permitted/protected phasings, based on both the results of field observations and models developed with simulation in previous chapters. The effects of bay length on the left-turn capacity under either the protected phase or subphase have also been incorporated in the capacity estimation procedures. The entire chapter is organized as follows:

The following section presents the operational procedures for protected left-turn capacity analysis, including required input variables, mathematical equations, and some key parameters computed from extensive field observations. Section 7.3 illustrates the relatively complex procedures for permitted capacity analysis, including the opposing queue length prediction, permitted saturation flow estimation, and a summary of key parameters calibrated from field studies. Sections 7.4 and 7.5 describe the application of both protected and permitted models for those protected/permitted and permitted/protected phasings, respectively. The core of both sections is to highlight the differences of the resulting capacity between a protected phase and subphase, as well as between a permitted phase and subphase. Comparisons of some critical variables such as the number of sneakers during an amber phase and between subphases also constitute the primary part of these two sections. Concluding comments along with some further research issues are the main focus of the last section.

Step 3: *Estimation of the number of left-turn sneakers during both the yellow and all red*

phases.

Note that the number of left-turn sneakers varies significantly from one location to

another, reflecting the local-specific driving characteristics.

Although this study has conducted extensive field studies, the analysis results do not show

any consistent pattern for the distribution of sneakers. One may have to conduct the estimation

based on local field observations, rather than from any other sources.

Step 4: *Capacity estimation with the following expression:*

$$C_{PT} = \left[\left[S_{PT}^* \cdot \frac{(g_{PT} - L_{PT})}{3600} \right] + N_s \right] \cdot K \tag{7.3}$$

where:

C_{PT}: the protected left-turn capacity (VPH)

S_{PT}^*: the adjusted saturation flow rate for left-turn (VPH)

g_{PT}: the protected green duration (second)

L_{PT}: the starting delay and time loss at the start of a protected green phase

N_s: the number of sneakers during the amber and all-red phases

K: the total number of cycles per hour

Note that the start-up delay or initial time loss is also a variable heavily dependent of local

driver behavior, and it often varies substantially even within the same region. The results from

our field observations are summarized below for reference:

$$\text{UGF} = \quad T_e - T_m \qquad\qquad \text{if } l_0 < l < l_1 \qquad\qquad\qquad (7.6.a)$$

$$\text{UGF} = \quad T_e + T_\gamma - \left[l/r_{to} \cdot a \right] \quad \text{if } l_1 < l < t_p\, r_{to}\, a \qquad (7.6.b)$$

$$\text{UGF} = \quad \text{Max} \left[T_1 + T_r - \frac{(l - t_p r_{to} \cdot a)}{r_{to} \cdot a} - t_p, \; 0 \right]$$

$$\text{if } l > \max (l_1,\, t_p\, r_{to}\, a)$$

where:

l: the left-turn bay length

T_l: green duration for left-turn movement per cycle

T_m: equals $(T_t + T_r + T_l) \cdot r_l/r_d$

T_t: green duration for through movement per cycle

T_r: red duration for both through and left-turn vehicles per cycle

r_l: left-turn arriving flow rate (VPH)

r_d: saturation discharging rate for left-turn flows (VPH)

a: the length occupied by per left-turn vehicle in queue

r_{to}:   arrival rate for the through movement during the non-platooning interval

t_p: time interval for the beginning of a red phase to the arrival of a platoon.

l_0: $\min \left[(L + T_r\, r_{lo} \cdot a) / (1 + r_{lo}/r_{to}),\, L \right]$

L: the maximum possible left-turn queue length, that equals

$$\left[T_p\, r_{lp} + (T_t + T_r + T_1 - T_p)\, r_{lo} \right] a$$

T_p: the total length of intervals during which vehicles from the upstream intersection are arriving in platoons

C: the cycle length at the target intersection

O: the offset between two neighboring intersections

P_p: signal progression factor, and equals $T_T - O$ if $T_T - 0 > 0$; or 1, if $T_t - 0 < 0$;

P_N: signal progression factor, and equals to $0 - T_t$ if $T_T - 0 < 0$; or 1, if $T_t - 0 > 0$.

Note that Eq. 7.7 provides an estimated queue length that is the longest among all opposing lanes. This is due to the fact that the existence of any queue vehicle in any of the opposing lane may prevent the exercise of permitted turns.

Step 2:   *Estimation of the total discharging time for the opposing queue size.*

To estimate the total queue discharging time, one may either conduct a field study regarding the average discharging headway for through movement or approximate its value from the sample field observations show in Figure 7.1.

Step 3:   *Computation of the effective permitted green time as follows:*

$$g_{PM}^{e} = g_{PM} - g_o \tag{7.8}$$

where:

g_{PM}^{e}:   the effective green time for permitted turns

g_{PM}:   the allocated green time for permitted turns

g_o: the total green time consumed for discharging the opposing queue vehicles

Step 4:   *Estimation of the permitted saturation flow rate with the following expression:*

$$S_{PM} = 180 \cdot (S)^{0.32} \cdot \left(\frac{t_{cr}}{5.0} \right)^{-0.63} \cdot \left(\frac{h}{2.0} \right)^{-0.69} \cdot \exp\left[\left(\frac{F_{OT}}{N_o} \right) \right]^{-0.0005}$$

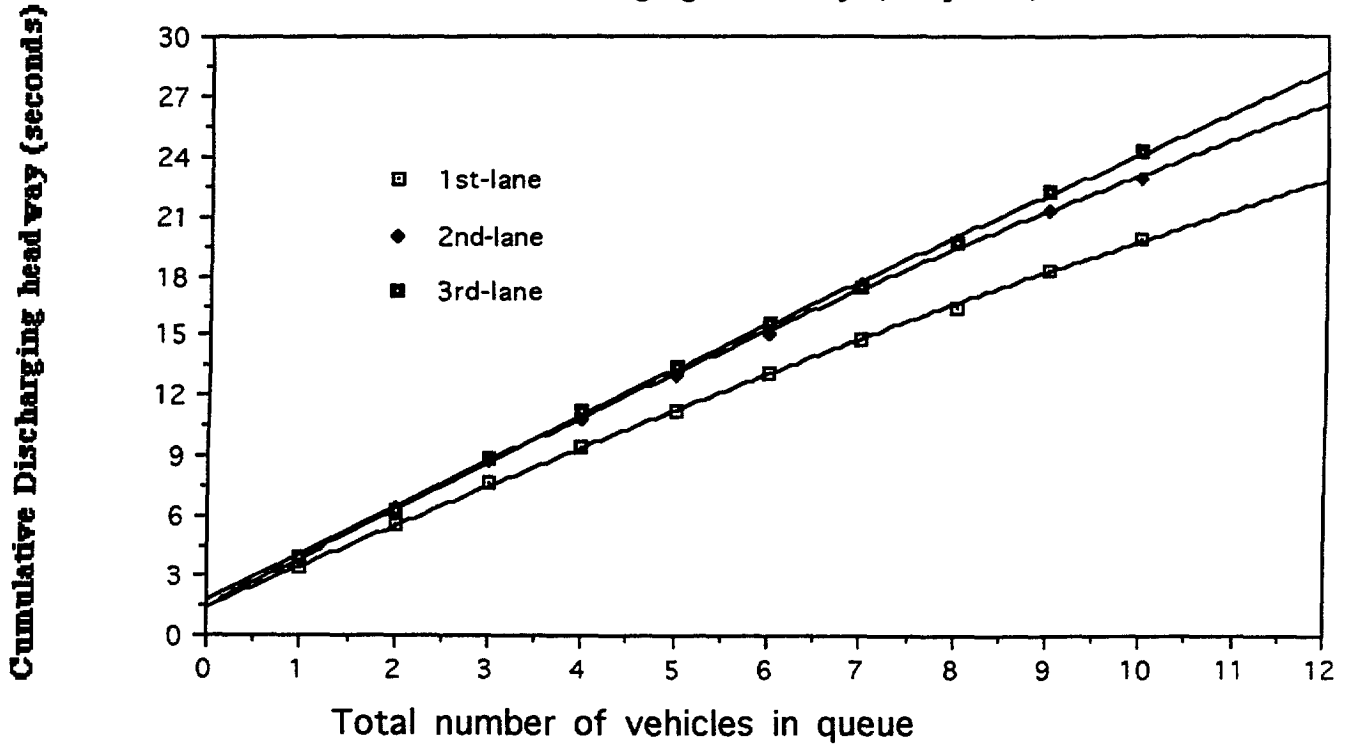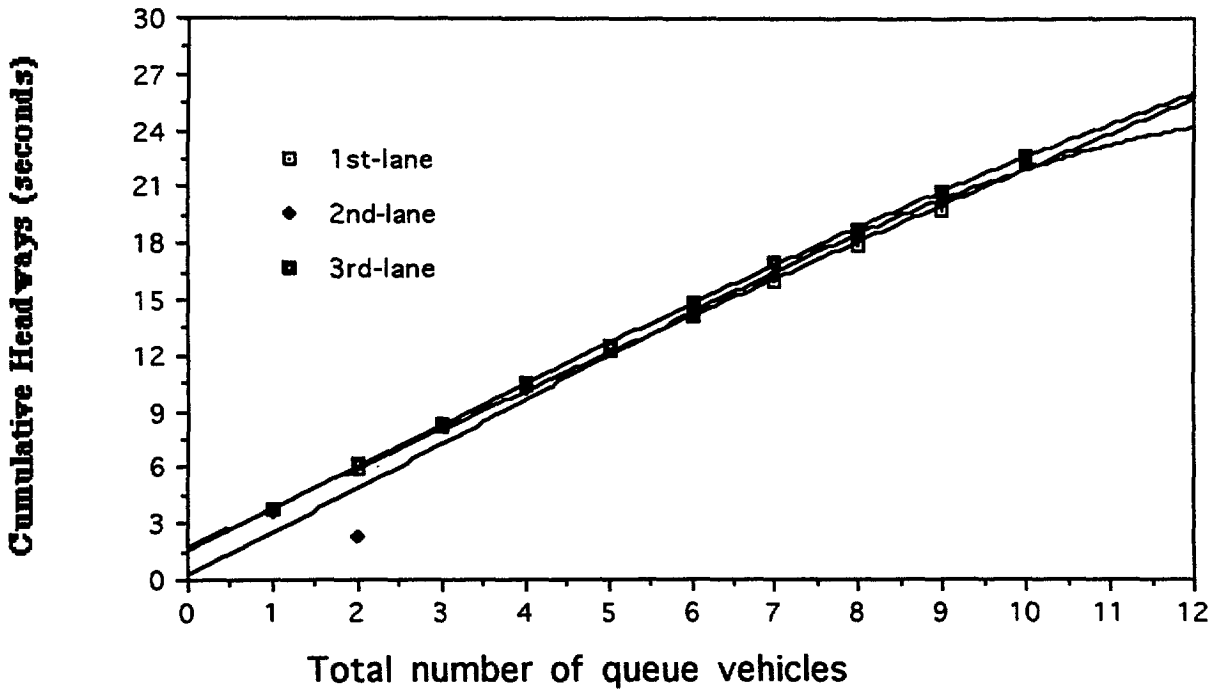# Figure 7-1(c): Field Observations of Through Queue Discharging Headway (Maryland)

Cumulative Discharging headway (seconds) vs Total number of vehicles in queue

- □ 1st-lane
- ◆ 2nd-lane
- ■ 3rd-lane

Figure 7-1(d): Field Observations of Through Queue Discharging Headway (Delaware)

Cumulative Headways (seconds) vs Total number of queue vehicles

- □ 1st-lane
- ◆ 2nd-lane
- ■ 3rd-lane

N_s^1:   the number of sneakers prior to the discharge of opposing queue vehicles (see

         Figure 7.2)

N_s^2:   the number of sneaker during the left-turn ambler and all-red phases

 K: the total number of cycles per hour

*Step 6:   Adjustment **of** the permitted left-turn capacity due to insufficient bay length.*

One can apply the same procedures as well as models in Section 7.2 for adjustment of

permitted capacity, if the left-turn movement is provided with a left-turn bay rather than a left-

turn lane.

7.4   **Procedures for Estimation of Protected/Permitted Capacity**

A protected/permitted (PT/PM) phase for left-turn is essentially a combination of a

protected subphase followed by a permitted subphase. In most such applications the left-turn

green duration is primarily allocated to the protected subphase, and only a very few vehicles are

allowed to filter through the remaining short permitted subphase. Consequently, the operational

characteristics of the protected subphase often do not have much impact on the left turns under

the following permitted phase. Hence, to estimate the left-turn capacity under PT/PM control,

one can take full advantage of procedures for both permitted and protected phasings, and

compute the capacity of its subphase under each type of control. A step-by-step description of

such procedures is presented below:

*Step 1:   Compute the saturation flow rate **for** the protected subphase with the same*

         procedures as in Section 7.2, including all necessary adjustments based on factors in
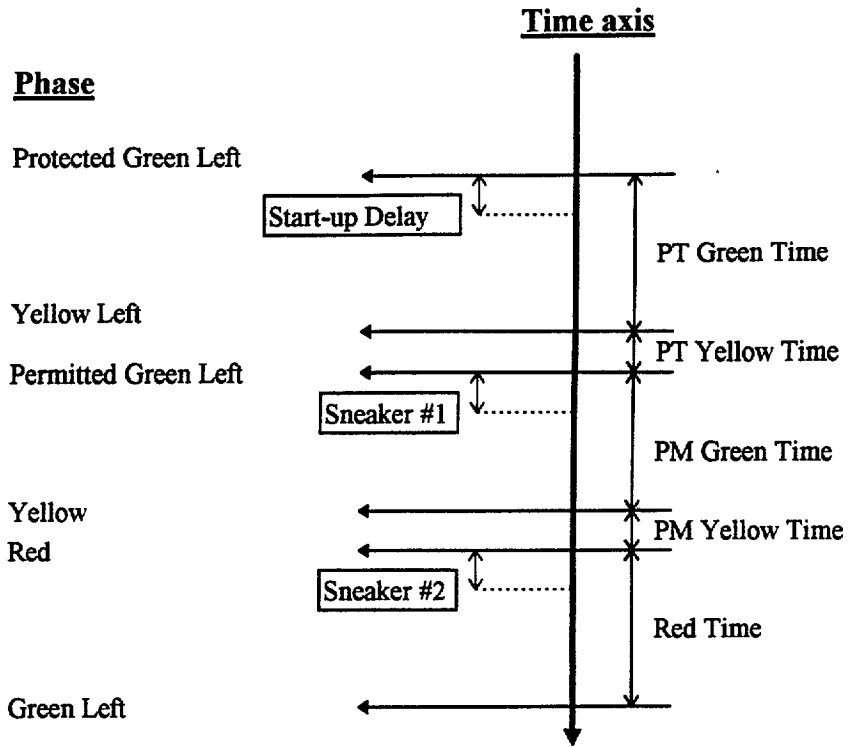
         the HCM.

Figure 7.2: A Graphical Illustration of A Protected/Permitted Phase

The procedures for analyzing such a signal phase are presented below.

Step 1: *Estimate the opposing queue length at the start of a permitted subphase with the*

following expression:

$$Q_M = Q^{0.8257} \cdot N^{0.1820} \cdot C^{-0.1569} \cdot (G/C)_u^{0.7089} \cdot P_P^{0.2782\delta} \cdot P_N^{0.2819(1-\delta)} \qquad (7.13)$$

where all variables in Eq. 7.13 have the same definitions as in Eq. 7.7. This equation, however, was calibrated with extensive simulated scenarios under PM/PT phasing.

Step 2: *Estimate the total discharging time for the opposing queue vehicles during the*

permitted subphase with the same procedures in Section 7.3.

Step 3: *Compute the capacity under the permitted subphase as follows:*

$$C_{PM}^s = \left[S_{PM}^s \cdot \left(\frac{g_{PM}^s}{3600} \right) + N_{s1}^s \right] \cdot K \qquad (7.14)$$

where N_{s1}^s is the number of left-turn sneakers prior to the discharge of opposing queue vehicles.

Step 4: *Compute the number of sneakers between the permitted and protected subphases (see*

Figure 7.3).

It has been observed that prior to the start of a protected subphase some left-turn vehicles may have moved over the stop-line and waited for gaps at the intersection. The size of such vehicles ranges from zero to two, varying substantially among different sites. Note that the start-up delay or time loss for the following protected subphase depends on the number of such vehicles, that, in turn affects its available capacity.

Step 5: *Computation of the start-up delay for the protected subphase.*

Based on the field studies at Michigan, one may classify the discharging patterns into the

following scenarios:

Scenario 1:   No car has moved over the stop line prior to the protected subphase

Scenario 2:   One car has moved over the stop line prior to the protected subphase

Scenario 3:   Two cars have moved over the stop line prior to the protected subphase.

Table 7.1 to 7.3 present some sample observations of such a distribution from the field sites in Michigan.

Table 7.1

Summary of left-turn discharging headways during the protected subphase

under Scenario 1 up to the 10th queue vehicle

unit = seconds

nth vehicle	1	2	3	4	5	6	7	8	9	10	State
Site 1	2.14	2.36	2.8	1.49	1.41	-	-	-	-	-	Michigan
Site 2	2.71	3.44	1.77	1.86	1.62	1.65	1.48	1.38	1.34	1.26	Michigan
Site 3	2.59	2.17	1.5	-	-	-	-	-	-	-	Michigan
Site 4	2.41	2.43	2.06	1.67	1.98	-	-	-	-	-	Michigan
Site 5	2.25	2.54	2.08	1.95	-	-	-	-	-	-	Michigan
Site 6	2.56	2.56	2.1	2.72	-	-	-	-	-	-	Michigan
Site 7	2.37	2.08	2.23	2.17	2.04	1.94	1.56	1.74	1.7	1.66	Maryland

Despite the limited field sites, one can clearly see the impacts of the sneaker size on the start-up delay of the first queued vehicle during the subsquent protected subphase. For instance, the start-up delay ranges from 2.14 to 2.59 seconds, under Scenario 1, but varies between 2.16 and 3.49 seconds under Scenario 2. The longest start-up delay apparently occurs in Scenario 3 where due to the presence of two sneakers. It takes the first queued vehicle from 2.39 to 3.72 seconds to cross the stop line.

Note that the above data may be used for reference and analysis if one cannot conduct field observations at the target site. However, considering the substantial difference on the start-up delay, that is due to the variation in driving characteristics, it will be essential to observe the distribution of those scenarios and use the following expression to compute both the average . sneakers between subphase transition and the actual time loss:

$$N_{s2} = \left[f_1 \cdot 0 + f_2 \cdot 1 + f_3 \cdot 2 \right] \qquad (7.14)$$

$$L_{PT}^{s} = \left[f_1 \cdot L_{PT}^{s1} + f_2 \cdot L_{PT}^{s2} + f_3 \cdot L_{PT}^{s3} \right] \qquad (7.15)$$

where:

f_1, f_2, and f_3:   the fractions of time per cycle have been observed to experience Scenarios 1 to 3, respectively.

L_{PT}^{s1}, L_{PT}^{s2}, and L_{PT}^{s3}:   the observed average start-up delay during the protected subphase under Scenarios 1 to 3, respectively

N_{s2}:   number of left-turn sneakers during the transition from a permitted to a protected subphase.

L_{PT}^{s}:   the average start-up time loss for a protected subphase under PM/PT control

Table 7.4 Key Variables Use in The Design of Experiments

Number of lane for left turn	1
Length of Exclusive left-turn lane	4000 ft
Number of opposing through lane	2
Link length to upstream intersection	1000 ft
Left-turn volume	800 vphpl
Opposing lane volume	300 - 1000 vphpl
Heavy vehicle percentage	0%
Desired speed	30 mph
Cycle length (both intersections)	60 sec
Green time for through vehicle (both intersections)	40 sec
Red time for through vehicle (both intersections)	14 sec
Yellow time (both intersections)	3 sec
Offset between both intersection	0 sec

Table 7.5 Comparison of Left-turn Capacity with Different Approaches

Case Study	Opposing Lane Volume (vphpl)	Left-turn Capacity		
		NETSIM	HCM	MODEL*
1	300	635	359	696
2	400	554	233	594
3	600	359	120	373
4	800	207	120	248
5	1000	108	120	162

* t_{cr} – 5.0 seconds and h = 2.0 seconds

To account for the impact of insufficient bay length on left-turn capacity, this study has also developed a hybrid model which allows traffic engineers to approximate the fraction of unusable left-turn green duration based on the arrival rates as well as distributions of both left-turn and through vehicles. The proposed bay length impact model considers both isolated intersections and interconnected networks where vehicles often arrive in platoons.

Finally, it should be noted that all proposed models are based on extensive simulation experiments along with field observations from 24 sites distributed in five states. Although the field studies are not sufficiently extensive to cover all possible scenarios, the results have constituted the basis for calibration of TRAF-NETSIM and validation of models developed from simulated data The integration of an effective simulation tool along with sample field data has led to the development of the above convenient procedures for direct estimation of left-turn capacity under various phasings.

Chapter 8: Conclusions

8.1   Summary of Research Work

To achieve a reliable estimation of left-turn capacity under various phase schemes has long been the concern of traffic researchers and engineers. In response to such a concern this study has focused on investigating the complex interactions between exclusive left-turn capacity and all associated factors, based on both field observations and extensive simulation experiments with TRAF-NETSIM. The research methodology, taking full advantage of a well-calibrated traffic simulation model, has been adopted due to the recognition of difficulties in having extensive field data from various states and the stochastic nature of traffic systems. With the proposed simulation-based method, one can fully capture the impacts of various critical factors on the left-turn operations, including traffic patterns and signal control at both the upstream and downstream intersections, and the distribution of various driving populations. The potential capacity variation under different driving populations or operational periods can also be explored with the simulation-based method.

To accommodate the need of various potential users, the research team has conducted this study along the following two lines: Direct estimation of left-turn capacity as well as its sensitivity with TRAF-NETSIM; and indirect capacity computation with a set of models developed from extensive simulated scenarios and field observations. With respect to the direct estimation, this research has yielded the following products:

·   A set of statistical procedures for calibration of both the start-up delay and
average discharge headway for TRAF-NESIM with limited field observations;

·   A set of statistical procedures for approximating the distribution of permitted left-turn headways for TRAF-NETSIM with available field data; and

·   Example procedures for direct computation of left-turn capacity under various phase schemes with TRAF-NETSIM.

For the indirect and sequential estimation of left-turn capacity, this project has yielded the following results:

·   A statistical model for left-turn saturation flow rate under a protected phase that allows traffic engineers to incorporate the locally-observed discharge headway in the capacity estimation;

·   A hybrid model for permitted saturation flow rate that accounts for the impacts of various critical factors, including:

the number of opposing lanes;

the distribution of opposing headways;

the opposing through flow rate;

the left-turn flow rate and heavy-vehicle percentage;

the distribution of queue discharge headways;

the signal control at both the upstream and downstream intersections; and

the quality of signal progression.

·   A set of statistical models for estimating the opposing queue size at the beginning of a permitted phase or subphase, and some empirical relations for approximation of the required discharge duration under a given queue size.

·   Two sets of analytical models to evaluate the impact of a provided bay length on

the left-turn capacity at congested isolated intersections and coordinated networks.

·   Some empirical relations from field observations to illustrate the impacts of

various driving patterns during the subphase transition on the capacity of the

subsequent subphase, such as between a permitted and a protected subphase in

permitted/protected control.

·   Four sets of operational procedures for computing the capacity of exclusive left

turns under protected, permitted, protected/permitted, and permitted/protected

phasings.

·   A hybrid model, integrating both the results from analytical derivations and

simulation experiments, for adjustment of the left-turn capacity under an

insufficient bay length.

As both the dynamic nature of traffic patterns and the discrepancy in driving behaviors

have significant impacts on the resulting capacity, one should first consider the application of a

well-calibrated simulation program for direct capacity estimation, if the available data are

sufficient for modeling the target intersection. The sequential procedures for capacity estimation

are the alternative for some one lacking either the experience of traffic simulation applications, or

the extensive local data to satisfy the input need of a microscopic program, such as TRAF-

NETSIM.

Regardless of the employed method, one should be recognized that *"capacity is not a*

constant, but a stochastic variable depending significantly on the distribution of driving

populations and resulting behavior " It is thus essential to incorporate the impact of driving

behavior factors in the capacity estimation. Neglecting such a vital local-specific factor, one may seriously under or over estimate the left-turn capacity, especially at intersections having either a permitted phase or subphase.

In summary, recognizing the prohibitive costs associated with having statistically sufficient field studies for model development, the research team has intentionally conducted this project along the direction that needs not to rely on the results or factors from extensive field observations in various states or locations, but to take full advantage of an effective simulation program with minimum locally available data. In addition, we have developed all those models based on both field data and simulated networks of these intersections, including the impacts of both downstream and upstream traffic patterns to realistically account for the traffic interactions in reality.

Based on all the above research accomplishments, we have summarized the sets of recommendations to Chapter 9 of the Highway Capacity Manual (HCM) in Table 8.1.

Table 8.1: A List of Recommendations to the HCM	
Recommendations	Reasons and/or strengths
1. Protected saturation flow rate model.	• Allow potential users to incorporate the observable, local-specific driving pattern in the estimation.
2. A hybrid permitted saturation flow rate model.	• Take advantage of both the analytical and statistical models. • Conveniently and effectively incorporate some critical traffic flow and driving behavioral factors in the estimation (e.g., distribution of queue discharge headways, the quality of signal progression, the distribution of headways in the opposing lanes).

3. A model for estimating the queue size on the opposing lanes.	• Provide an efficient and effective way for computing the effective green time. • Include both the progression quality and the upstream signal settings in the queue length estimation. • Consider the signal control at both the target and upstream intersections on the queue size estimation.
4. A hybrid model for assessing the impact of a given bay length on the resulting left-turn capacity.	• Enable the potential users to analytically estimate the impact of various bay lengths on the left-turn capacity; • Capable of estimating the bay length impacts at both isolated and coordinated intersections; • Conveniently incorporate some intractable but vital relations among the bay length, left-turn capacity, and key traffic characteristic factors through a hybrid modelling expression. • The procedures to assess the impact of a given bay length on the resulting capacity are not available in the current HCM.
5 A set of empirical relations to discuss the impacts of various driving patterns during the subphase transition on the subsequent subphase capacity.	• Provide some preliminary assessment of the potential impacts, due to the driving behavior discrepancy, on the protected/permitted and permitted/protected capacities. • The current HCM procedures have not addressed the impact of driving patterns during the subphase transition on the protected/permitted and permitted/protected capacities.
6 A set of statistical procedures for calibrating the discharge headways and start-up delay from field data.	• Offer a set of statistically rigorous steps for field data analysis. • Set up the guidelines for incorporating the field data in a simulation program for capacity analysis.
7 A set of procedures for direct estimation of intersection capacity with simulation.	• Enable potential users familiar with simulation applications to directly estimate the intersection capacity with any reliable simulation program.

8.2   Further Research Needs

The research team has fully recognized that to promote the above simulation-based methods for capacity estimation, many remain to be done. For direct estimation of capacity with simulation, research needs include:

- A user-friendly interface in TRAF-NETSIM designed specifically for the purpose of capacity estimation;

- **A** statistical module for automated parameter calibration with available field observations; and

- A reliable gap distribution model for permitted left turns under various opposing lanes.

    The embedded statistical module should have the flexibility to employ different methods for field observations collected at different levels of detail, and produce statistically robust parameters for simulation applications.

For the method of sequential computation, research needs for left-turn operations include:

- A reliable analytical or hybrid model for estimating the approach vehicle delay under various signal phasing plans;

- Empirical models or statistical formulations for reliable and convenient estimation of the impact due to the differences in driving behavior during the subphase transition on the capacity of a subsequent subphase;

- A set of systematic procedures to estimate the optimal bay length under given traffic conditions;

·   A hybrid model or set of statistical equations to estimate the impact of various bay

lengths of double-lanes on the left-turn capacity; and

·   Field evaluation or calibration of the proposed procedures and models for capacity

adjustment due to an insufficient bay length.